Identification of *rfk-1*, a Meiotic Driver Undergoing RNA Editing in *Neurospora*

Nicholas A. Rhoades,* Austin M. Harvey,*,[1] Dilini A. Samarajeewa,*,[1] Jesper Svedberg,[†] Aykhan Yusifov,* Anna Abusharekh,* Pennapa Manitchotpisit,* Daren W. Brown,[‡] Kevin J. Sharp,* David G. Rehard,[§,] Joshua Peters,* Xavier Ostolaza-Maldonado,* Jackson Stephenson,* Patrick K. T. Shiu,[§] Hanna Johannesson,[†] and Thomas M. Hammond*,[2]**

*School of Biological Sciences, Illinois State University, Normal, Illinois 61790, [†]Department of Organismal Biology, Uppsala University, Norbyvägen 18D, 752 36 Uppsala, Sweden, [‡]Mycotoxin Prevention and Applied Microbiology, National Center for Agricultural Utilization Research, U.S. Department of Agriculture, Agricultural Research Service, Peoria, Illinois 61604, [§]Division of Biological Sciences, University of Missouri, Columbia, Missouri 65211, and **Department of Biology, University of Iowa, Iowa 52242

ABSTRACT *Sk-2* is a meiotic drive element that was discovered in wild populations of *Neurospora* fungi over 40 years ago. While early studies quickly determined that *Sk-2* transmits itself through sexual reproduction in a biased manner via spore killing, the genetic factors responsible for this phenomenon have remained mostly unknown. Here, we identify and characterize *rfk-1*, a gene required for *Sk-2*-based spore killing. The *rfk-1* gene contains four exons, three introns, and two stop codons, the first of which undergoes RNA editing to a tryptophan codon during sexual development. Translation of an unedited *rfk-1* transcript in vegetative tissue is expected to produce a 102-amino acid protein, whereas translation of an edited *rfk-1* transcript in sexual tissue is expected to produce a protein with 130 amino acids. These findings indicate that unedited and edited *rfk-1* transcripts exist and that these transcripts could have different roles with respect to the mechanism of meiotic drive by spore killing. Regardless of RNA editing, spore killing only succeeds if *rfk-1* transcripts avoid silencing caused by a genome defense process called meiotic silencing by unpaired DNA (MSUD). We show that *rfk-1*'s MSUD avoidance mechanism is linked to the genomic landscape surrounding the *rfk-1* gene, which is located near the *Sk-2* border on the right arm of chromosome III. In addition to demonstrating that the location of *rfk-1* is critical to spore-killing success, our results add to accumulating evidence that MSUD helps protect *Neurospora* genomes from complex meiotic drive elements.

KEYWORDS Genetics of Sex; meiotic drive; meiotic silencing; RNA editing; spore killing; transmission ratio distortion

IN eukaryotic organisms, alleles of nuclear genes are typically inherited in a Mendelian manner. However, some genes possess the ability to improve their own transmission rate through meiosis at the expense of a competing locus. These "selfish" genes are often referred to as meiotic drive elements (Zimmering *et al.* 1970). The genomic conflict caused by meiotic drive elements may impact processes ranging from gametogenesis to speciation (Lindholm *et al.* 2016). Meiotic drive elements are found across the eukaryote tree of life (Burt and Trivers 2008; Bravo Núñez *et al.* 2018), and classic examples include *SD* in fruit flies (Larracuente and Presgraves 2012), the *t*-complex in mice (Lyon 2003; Sugimoto 2014), and *Ab10* in *Zea mays* (Rhoades 1952; Kanizay *et al.* 2013). In the fungal kingdom, the known meiotic drive elements achieve biased transmission through spore killing (Raju 1994) and a handful of spore killer systems have been studied in detail. While the prion-based spore-killing mechanism of *het-s* in *Podospora anserina* is well characterized (Dalstra *et al.* 2003; Saupe 2011), the mechanisms by which other fungal meiotic drive elements kill spores are mostly unknown [*e.g.*, see Grognet *et al.* (2014), Hu *et al.* (2017), and Nuckolls *et al.* (2017)].

Two fungal meiotic drive elements have been identified in the fungus *Neurospora intermedia* (Turner and Perkins 1979). This species is closely related to the genetic model *N. crassa* (Davis 2000), and the mating processes in both fungi are essentially identical. Mating begins with the

doi: https://doi.org/10.1534/genetics.119.302122
Manuscript received July 13, 2018; accepted for publication March 21, 2019; published Early Online March 27, 2019.
Supplemental material available at Figshare: https://doi.org/10.25386/genetics.7836692.
[1]These authors contributed equally to this work.
[2]Corresponding author: School of Biological Sciences, Illinois State University, 346 Science Laboratory Bldg., Normal, IL 61790. E-mail: tmhammo@ilstu.edu

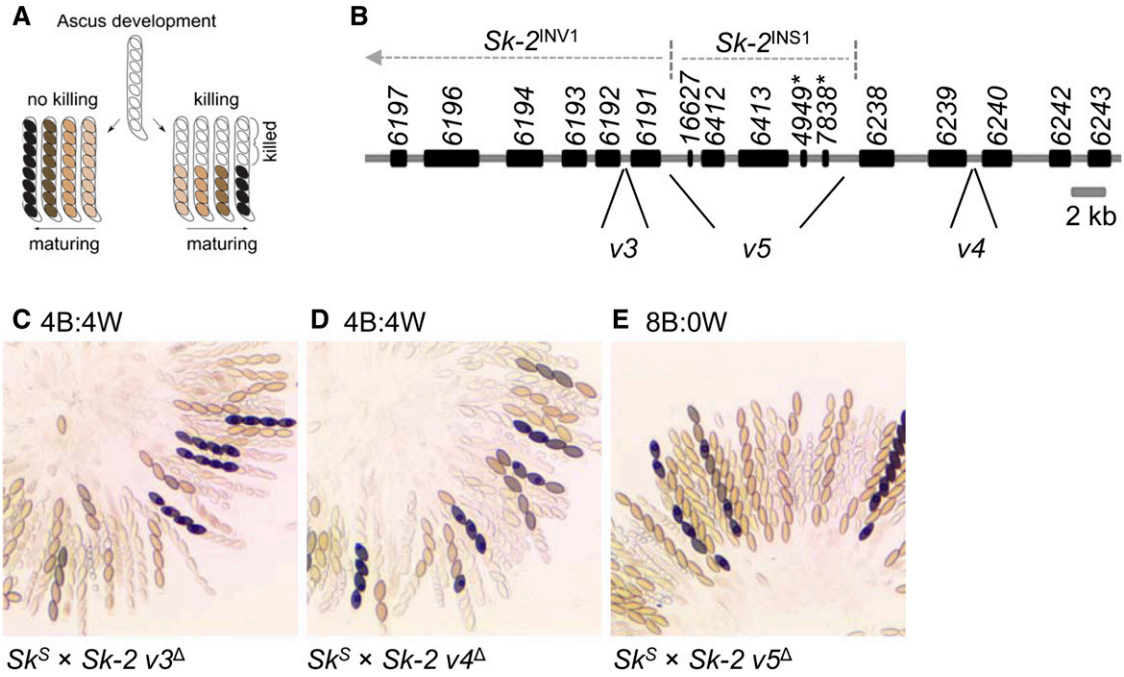

Figure 1 *Sk-2*^{INS1} harbors a genetic element required for spore killing. (A) The diagram illustrates phenotypic differences between spore killing and normal ascus development. Asci that have undergone spore killing contain four black and four white ascospores. Viable ascospores may appear tan, brown, or black, depending on their level of maturity. (B) Annotation of the *rfk-1* region as described by Harvey *et al.* (2014). Genes and pseudogenes are depicted as black rectangles. Gene names (*e.g.*, *6197*) are listed above the rectangles. Pseudogene names are appended with an asterisk. Labels *v3*, *v4*, and *v5* mark DNA intervals of the *rfk-1* region, which were deleted and replaced with an *hph* selectable marker. (C–E) The images depict asci from crosses between *Sk*^{S} and *Sk-2* strains lacking different intervals of the *rfk-1* region. The predominant phenotype of the asci produced by each cross is listed above its image. Crosses are as follows: (C) F2-23 × ISU-3023, (D) F2-23 × ISU-3017, and (E) F2-23 × ISU-3029. B, black; W, white.

fertilization of an immature fruiting body (protoperithecium) by a mating partner of the opposite mating type. After fertilization, the protoperithecium develops into a mature fruiting body called a perithecium. The nuclei from each parent multiply within the developing perithecium, and a single nucleus from each parent is sequestered into a tube-like meiotic cell (Raju 1980). Meiosis begins with the fusion of parental nuclei and ends with the production of four recombinant daughter nuclei. Each recombinant nucleus proceeds through a single round of mitosis, resulting in a total of eight nuclei in the meiotic cell. A process known as ascosporogenesis then constructs cell walls and membranes around each nucleus to produce sexual spores called ascospores. Maturing ascospores accumulate a dark pigment and develop into the shape of a spindle; thus, at the end of ascosporogenesis, a mature meiotic cell appears to contain eight miniature black American footballs (Figure 1A). The meiotic cells also serve as ascospore sacs (asci) and a single perithecium can produce hundreds of asci, each derived from a unique meiotic event.

During an effort in the 1970s to collect and characterize *Neurospora* isolates from around the world, Turner and Perkins discovered pairs of compatible mating partners that did not produce asci with eight viable ascospores (Perkins 1974; Turner and Perkins 1979). This outcome was more common when crosses were performed between isolates from widely separated populations, and in some cases, the abnormal asci were attributed to heterozygosity of chromosome rearrangements between mating partners. However, for a few isolates of *N. intermedia*, asci with atypical phenotypes were found to be due to chromosomal factors called *Spore killer-2* (*Sk-2*) and *Spore killer-3* (*Sk-3*). *Sk-2* and *Sk-3* are not single genes; rather, they are complexes of genes that span ~30 cM of chromosome III and are transmitted through meiosis as single units due to a recombination suppression mechanism thought to be enforced by inversions (Turner and Perkins 1979; Campbell and Turner 1987; Hammond *et al.* 2012; Harvey *et al.* 2014; Svedberg *et al.* 2018). Unlike standard genetic elements, which display a Mendelian transmission rate of 50% through sexual reproduction, *Sk-2* and *Sk-3* are transmitted at levels approaching 100% (Turner and Perkins 1979). This biased transmission occurs because *Sk-2* and *Sk-3* kill ascospores that do not inherit resistance to spore killing (Raju 1979; Turner and Perkins 1979). For example, in *Sk-2* × *Spore killer*-sensitive (*Sk*^{S}) crosses, asci with four black ascospores and four clear ("white") ascospores are produced (Figure 1A). This phenotype can be symbolized as 4B:4W. The four black ascospores are typically viable and nearly always of the *Sk-2* genotype, while the four white ascospores are inviable and presumed to be of the *Sk*^{S} genotype. The same phenomenon occurs in *Sk-3* × *Sk*^{S} crosses, except that the four black ascospores are of the *Sk-3* genotype.

Although the Spore killers have not yet been detected in wild isolates of *N. crassa*, *Sk-2* and *Sk-3* have been

Table 1 Strains used in this study

Name (alias)	Genotype[a]
F2-19	*rid*; *fl*; *Sk-2 A*
F2-23 (RTH1005.1)	*rid*; *fl A*
F2-26 (RTH1005.2)	*rid*; *fl a*
FGSC 1766	*N. intermedia A*
FGSC 1767	*N. intermedia a*
FGSC 7426	*N. intermedia Sk-2 A*
ISU-3017 (RKS2.1.2)	*rid*$^{?}$; *Sk-2 leu-1 v4*$^{\Delta}$*::hph*; *mus-51*$^{?}$ *a*
ISU-3023 (RKS1.1.6)	*rid*$^{?}$; *Sk-2 leu-1 v3*$^{\Delta}$*::hph*; *mus-51*$^{?}$ *a*
ISU-3029 (RKS3.2.5)	*rid*; *Sk-2 leu-1 v5*$^{\Delta}$*::hph*; *mus-51*$^{\Delta}$*:bar a*
ISU-3036 (RTH1623.1)	*rid*; *fl*; *sad-2*$^{\Delta}$*::hph A*
ISU-3037 (RTH1623.2)	*rid*; *fl*; *sad-2*$^{\Delta}$*::hph a*
ISU-3211 (RTH1158.8)	*rid*; *Sk-2 rsk*$^{\Delta}$*::hph rfk-1*^{3211}; *mus-51*$^{\Delta}$*::bar a*
ISU-3212 (RTH1158.13)	*rid*; *Sk-2 rsk*$^{\Delta}$*::hph rfk-1*^{3212} *a*
ISU-3213 (RTH1158.24)	*rid*; *Sk-2 rsk*$^{\Delta}$*::hph rfk-1*^{3213} *a*
ISU-3214 (RTH1158.34)	*rid*; *Sk-2 rsk*$^{\Delta}$*::hph rfk-1*^{3214}; *mus-51*$^{\Delta}$*::bar A*
ISU-3215 (RTH1158.35)	*rid*; *Sk-2 rsk*$^{\Delta}$*::hph rfk-1*^{3215} *a*
ISU-3216 (RTH1158.44)	*rid*; *Sk-2 rsk*$^{\Delta}$*::hph rfk-1*^{3216} *a*
ISU-3222 (RTH1249.14)	*rid*; *Sk-2 rfk-1*^{3211}; *mus-51*$^{\Delta}$*::bar a*
ISU-3223 (RTH1294.17)	*Sk-2 leu-1*; *mus-51*$^{\Delta}$*::bar A*
ISU-3224 (HAH8.1.3)	*rid his-3*$^{+}$*::AH4*$^{Sk\text{-}2}$*-hph*; *A*
ISU-3228 (HAH10.1.1)	*rid his-3*$^{+}$*::AH6*$^{Sk\text{-}2}$*-hph*; *A*
ISU-3243 (HAH16.1.1)	*rid his-3*$^{+}$*::AH14*$^{Sk\text{-}2}$*-hph a*
ISU-3311 (RDS1.1)	*Sk-2 leu-1 v31*$^{\Delta}$*::hph*; *mus-51*$^{\Delta}$*::bar A*
ISU-3313 (RDS2.3)	*Sk-2 leu-1 v32*$^{\Delta}$*::hph*; *mus-51*$^{\Delta}$*::bar A*
ISU-3315 (RDS3.9)	*Sk-2 leu-1 v33*$^{\Delta}$*::hph a*
ISU-3318 (RDS4.8)	*Sk-2 leu-1 v34*$^{\Delta}$*::hph A*
ISU-3321 (RDS5.9)	*rid*; *Sk-2 leu-1 v35*$^{\Delta}$*::hph*; *mus-51*$^{\Delta}$*::bar a*
ISU-3478 (RDS13.9.1)	*rid*; *Sk-2 v37*$^{\Delta}$*::hph*; *mus-51*$^{\Delta}$*::bar A*
ISU-3482 (RDS14.4.2)	*rid*; *Sk-2 v38*$^{\Delta}$*::hph A*
ISU-3483 (RDS15.1.1)	*rid*; *Sk-2 v39*$^{\Delta}$*::hph A*
ISU-3485 (RDS16.4.1)	*rid*; *Sk-2 v40*$^{\Delta}$*::hph A*
ISU-3656 (HAH42.1)	*rid his-3*$^{+}$*::AH30*$^{Sk\text{-}2}$*-hph A*
ISU-3658 (HAH43.1)	*rid his-3*$^{+}$*::AH31*$^{Sk\text{-}2}$*-hph A*
ISU-3660 (HAH44.1)	*rid his-3*$^{+}$*::AH32*$^{Sk\text{-}2}$*-hph A*
ISU-4269 (RAH64.1.1)	*rid his-3*$^{+}$*::AH37*$^{Sk\text{-}2}$*-hph*; *mus-52*$^{\Delta}$*::bar a*
ISU-4271 (RAH63.1.2)	*rid his-3*$^{+}$*::AH36*$^{Sk\text{-}2}$*-hph*; *mus-52*$^{\Delta}$*::bar A*
ISU-4273 (HNR12.6.1)	*rid his-3*$^{+}$*::AH36*$^{Sk\text{-}2}$*-hph A*
ISU-4275 (HNR10.4.2)	*rid his-3*$^{+}$*::AH36*^{3211}*-hph A*
ISU-4344 (RAY1.13)	*rid*; *Sk-2 v140*$^{\Delta}$*::hph*; *mus-51*$^{\Delta}$*::bar a*
ISU-4348 (RAY6.5)	*rid*; *fl*; *v150*$^{\Delta}$*::hph A*
ISU-4551 (RNR29.1)	*rid his-3*$^{+}$*::AH36*$^{Sk\text{-}2[G27945A]}$*-hph*; *mus-52*$^{?}$ *A*
ISU-4552 (RNR28.1)	*rid his-3*$^{+}$*::AH36*$^{Sk\text{-}2[G27972A]}$*-hph*; *mus-52*$^{?}$ *A*
ISU-4553 (RNR27.1)	*rid his-3*$^{+}$*::AH36*$^{Sk\text{-}2[G28052A]}$*-hph*; *mus-52*$^{?}$ *A*
ISU-4554 (RNR26.1)	*rid his-3*$^{+}$*::AH36*$^{Sk\text{-}2[G28104A]}$*-hph*; *mus-52*$^{?}$ *A*
ISU-4555 (RNR25.1)	*rid his-3*$^{+}$*::AH36*$^{Sk\text{-}2[G28300A]}$*-hph*; *mus-52*$^{?}$ *A*
ISU-4556 (RNR30.1)	*rid his-3*$^{+}$*::AH36*$^{Sk\text{-}2[G28326A]}$*-hph*; *mus-52*$^{?}$ *A*
ISU-4557 (RNR129.1.3)	*rid*; *Sk-2 v199*$^{\Delta}$*::hph-ccg-1*(P)-ATG; *mus51*$^{?}$ *A*
ISU-4559 (RNR108.1.12)	*rid*; *fl*; *ncu06238*$^{\Delta}$*::hph mus-52*$^{\Delta}$*::bar a*
ISU-4561 (RNR109.3.2)	*rid*; *Sk-2 ncu06238*$^{\Delta}$*::hph*; *mus51*$^{\Delta}$*::bar A*
ISU-4562 (HNR92.1)	*rid*; *Sk-2 v160*$^{\Delta}$*::nat1*; *mus-51*$^{\Delta}$*::bar a*
ISU-4563 (HNR100.11.1)	*rid*; *Sk-2 v140*$^{\Delta}$*::hph*; *mus-51*$^{\Delta}$*::bar a*
ISU-4576 (HAA108.1.1)	*rid*; *Sk-2 v214*$^{\Delta}$*::hph-ccg-1*(P)-ATGT; *mus-51*$^{\Delta}$ *A*
ISU-4584 (HAA117.1.1)	*rid*; *Sk-2 v221*$^{\Delta}$*::hph-ccg-1*(P)-TAA; *mus-51*$^{\Delta}$ *A*
P8-42	*rid*; *mus-51*$^{\Delta}$*::bar a*
P8-43	*rid*; *mus-52*$^{\Delta}$*::bar A*
P15-53 (RTH1122.22)	*rid*; *Sk-2*; *mus-51*$^{\Delta}$*::bar A*

[a] The *rid*$^{?}$, *mus-51*$^{?}$, and *mus-52*$^{?}$ designations are used if the genotype has not been determined for the indicated allele. Genotypes of critical alleles were determined by PCR and/or lineage analysis.

Table 2 Interval positions

Name	Start	Stop
Miscellaneous intervals of the 45-kb *rfk-1* region		
Sk-2^{INS1}	18,118	29,151
rfk-1 coding	28,264	28,968/29,106
Repetitive[a]	28,384	28,722
Intervals deleted from the 45-kb *rfk-1* region		
v3	15,640	15,664
v4	36,166	36,426
v5	18,042	28,759
v31	18,042	21,464
v32	18,042	25,268
v33	18,042	26,951
v34	18,042	27,667
v35	25,837	28,759
v37	27,242	28,759
v38	27,602	28,759
v39	28,126	28,759
v40	27,602	28,198
v140	29,381	29,401
v160	27,740	29,401
v175	29,489	31,883
v199	28,131	28,263
v214	28,131	28,263
v221	28,131	28,263
Intervals transferred from the 45-kb *rfk-1* region to *Sk*^{S}		
AH4	16,579	22,209
AH6	19,408	25,648
AH14	25,632	28,324
AH30	27,528	29,702
AH31	27,900	29,702
AH32	28,304	29,702
AH36	27,900	29,380
AH37	27,900	29,512

The coordinates of each interval correspond to the GenBank sequence KJ908288.1.
[a] Contains repeats of a 46–48-bp sequence.

introgressed into this species for genetic analysis. Introgression of *Sk-2* and *Sk-3* has allowed resistance to spore killing to be discovered in natural populations of *N. crassa* (Turner and Perkins 1979; Turner 2001). An *Sk-2*-resistant isolate from Louisiana [Fungal Genetics Stock Center (FGSC) 2222] was found to carry a resistant version of a gene whose function is best described by its name: *resistant to Spore killer* (*rsk*). Crosses of *rsk*^{LA} × *Sk-2*, where *rsk*^{LA} is the allele of *rsk* carried by FGSC 2222, produce asci with an 8B:0W phenotype because ascospores inherit either *rsk*^{LA} or *Sk-2*, and both alleles are sufficient for resistance to *Sk-2*-based spore killing (Hammond *et al.* 2012). Discovery of *rsk*^{LA} made identifying other *rsk* alleles possible, some of which do not provide resistance to the known Spore killers. For example, the Oak Ridge *rsk* allele (*rsk*^{OR}), typical of most laboratory strains of *N. crassa*, is resistant to neither *Sk-2* nor *Sk-3*. Additionally, some *rsk* alleles confer resistance to *Sk-3* but not *Sk-2*. An example is *rsk*^{PF5123}, found in an *N. intermedia* isolate from French Polynesia. *Sk-2* and *Sk-3* also carry resistant versions of *rsk*, referred to as *rsk*$^{Sk\text{-}2}$ and *rsk*$^{Sk\text{-}3}$, respectively. Crosses homozygous for *Sk-2* (*i.e.*, *Sk-2* × *Sk-2*) or *Sk-3* produce asci with an 8B:0W phenotype because each ascospore inherits a

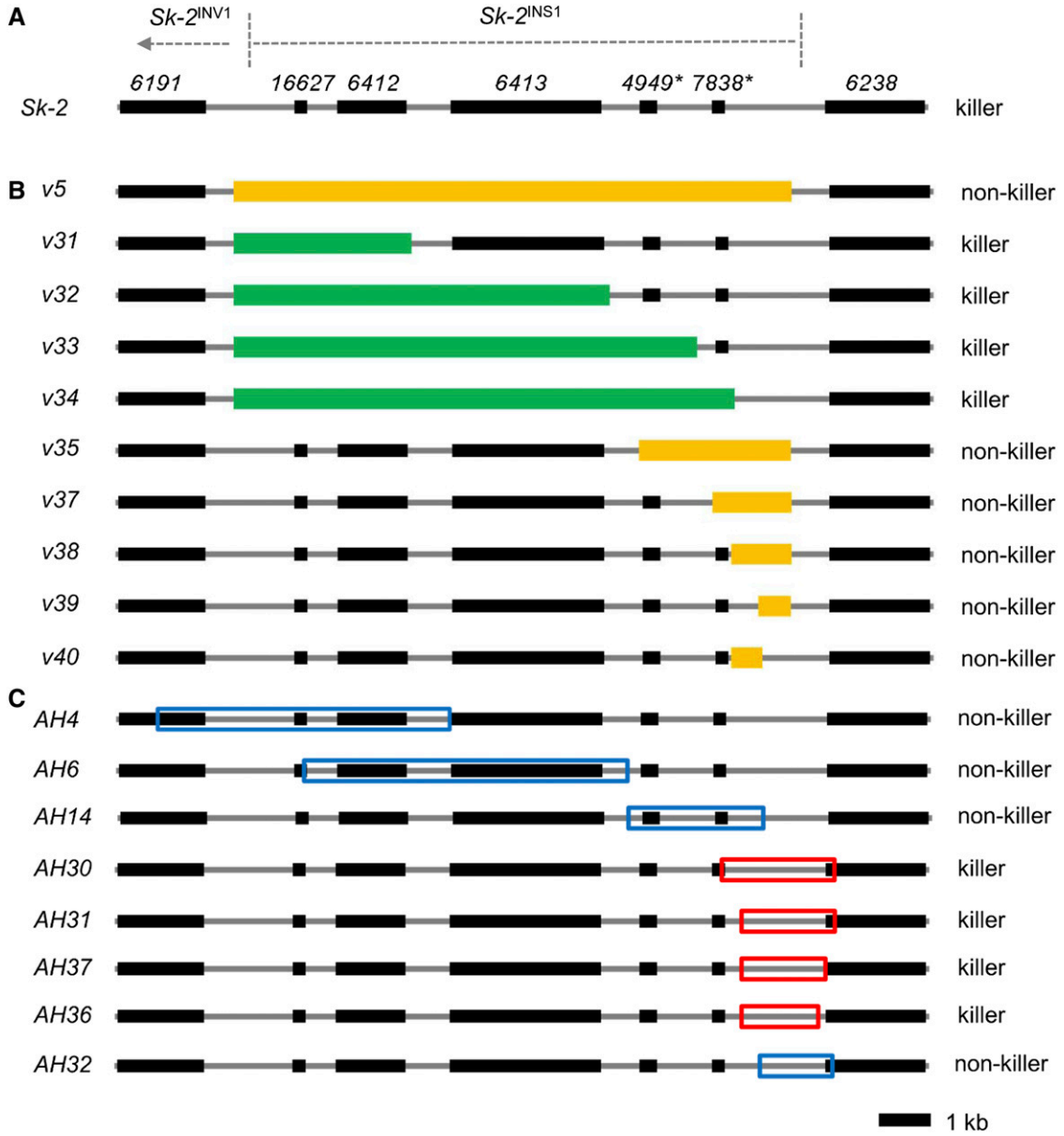

Figure 2 Deletion and insertion maps. (A) A diagram of *Sk-2*^{INS1} and its immediate neighbors. (B) Various intervals of *Sk-2*^{INS1} were deleted and replaced with *hph*. For convenience, each interval was named according to its deletion vector (*e.g.*, interval *v5* is named after deletion vector *v5*). Mango rectangles mark intervals that disrupt spore killing upon deletion. Green rectangles mark intervals that do not disrupt spore killing when deleted. (C) Eight intervals of *Sk-2*^{INS1} were transferred to the *his-3* locus of an *Sk*^{S} strain. Intervals were labeled according to the name of the plasmid used to clone each interval (*e.g.*, interval *AH4* is named after plasmid pAH4). Red and blue boxes mark killer (*i.e.*, abortion-inducing) and nonkiller intervals, respectively.

resistant *rsk* allele. In contrast, heterozygous crosses between different Spore killers (*e.g.*, *Sk-2* × *Sk-3*) produce asci with a 0B:8W phenotype (Turner and Perkins 1979) because each ascospore inherits either *rsk*$^{Sk-2}$ or *rsk*$^{Sk-3}$, but not both (*rsk*$^{Sk-2}$ ascospores are killed by *Sk-3*, while *rsk*$^{Sk-3}$ ascospores are killed by *Sk-2*).

The Killer-Neutralization (KN) model has been proposed to explain how *Sk-2* and *Sk-3* achieve biased transmission through sexual reproduction (Hammond *et al.* 2012). In this model, *Sk-2* and *Sk-3* each use a resistance protein and a killer protein (or nucleic acid), and both proteins are active throughout meiosis and ascosporogenesis; thus, in an *Sk*^{S} × *Sk-2* (or *Sk-3*) cross, both the resistance protein and the killer protein diffuse freely throughout the meiotic cell during early stages of meiosis. This unrestricted movement of both proteins allows the resistance protein to neutralize the killer throughout the cell. However, once ascospores are separated from the cytoplasm by ascospore delimitation, the resistance protein becomes restricted to the ascospores that produce it (*i.e.*, *Sk-2* ascospores). Ascospores that do not carry a resistant version of *rsk* (*i.e.*, *Sk*^{S} ascospores) are subsequently killed. This model requires the killer to move

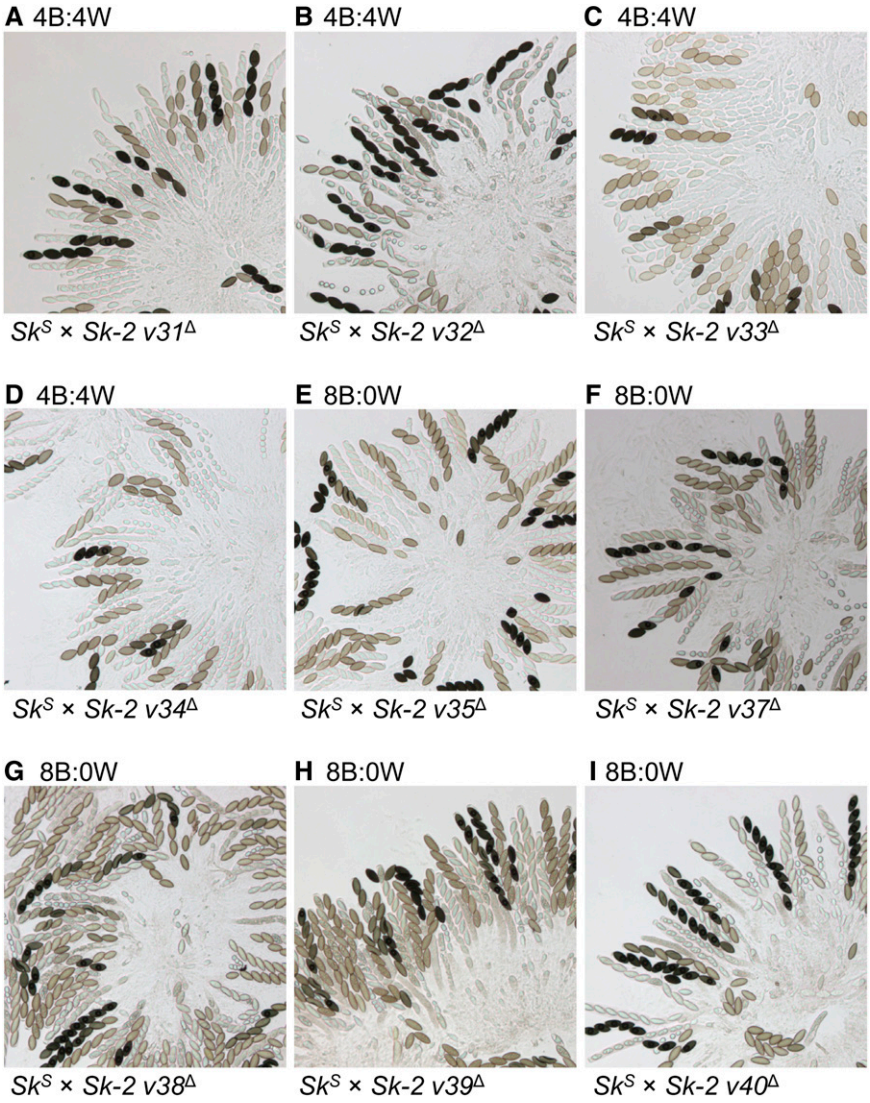

Figure 3 Deletion of a genetic element between pseudogene *7838** and the right border of *Sk-2*^{INS1} eliminates spore killing. (A–I) The images depict asci from crosses between an *Sk*^{S} strain and an *Sk-2* mating partner. Each *Sk-2* mating partner has been deleted of a different subinterval of *v5*. Crosses are as follows: (A) F2-26 × ISU-3311, (B) F2-26 × ISU-3313, (C) F2-23 × ISU-3315, (D) F2-26 × ISU-3318, (E) F2-23 × ISU-3321, (F) F2-26 × ISU-3478, (G) F2-26 × ISU-3482, (H) F2-26 × ISU-3483, and (I) F2-26 × ISU-3485. B, black; W, white.

between ascospores after ascospore delimitation. Alternatively, the killer may have a long half-life that allows it to remain functional in sensitive ascospores after ascospore delimitation.

Evidence for the KN model is seen in the outcome of *Sk*^{S} × *Sk-2 rsk*$^{\Delta Sk\text{-}2}$ crosses, where the latter strain has been deleted of its *rsk* allele. These crosses do not produce ascospores. Instead, *Sk*^{S} × *Sk-2 rsk*$^{\Delta Sk\text{-}2}$ crosses produce asci that abort meiosis before ascospore production (Hammond *et al.* 2012). Meiotic cells of these crosses lack a resistant RSK, which likely causes the killing process to begin early in meiosis (at the ascus level) rather than during ascosporogenesis (at the ascospore level). The KN model is also supported by the existence of different *rsk* alleles. For example, previous studies have demonstrated that the sequence of RSK is the most important factor toward determining which killer it neutralizes, suggesting that RSK and the killer may interact by a "lock-and-key" mechanism (Hammond *et al.* 2012). However, to test this hypothesis, the killer must first be identified.

As described above, *Sk*^{S} × *Sk-2 rsk*$^{\Delta Sk\text{-}2}$ crosses fail to produce viable ascospores, presumably because the killer protein is present and the resistance gene is not. We recently used this ascospore production defect to screen for mutations that disrupt spore killing (Harvey *et al.* 2014). Specifically, we fertilized an *Sk*^{S} mating partner with mutagenized *Sk-2 rsk*$^{\Delta Sk\text{-}2}$ conidia (asexual spores that also function as fertilizing propagules), reasoning that only an *Sk-2 rsk*$^{\Delta Sk\text{-}2}$ conidium that was mutated in a gene "*r*equired *f*or *k*illing" (*rfk*) would allow viable ascospores to be produced. With this method, we isolated six *rfk* mutants (ISU-3211 through ISU-3216). Complementation analysis of these mutants suggested that they are all mutated at the same locus, which was subsequently named *rfk-1* and mapped to a 45-kb region within *Sk-2* on chromosome III.

In this study, we identify and characterize *rfk-1*. Our results indicate that *rfk-1* is required for spore killing and that it is located next to the right border of *Sk-2*. This location allows it to escape silencing caused by a genome defense process called meiotic silencing by unpaired DNA (MSUD) (Shiu *et al.* 2001). We propose a model of *rfk-1* gene structure that includes four exons, three introns, and a coding region for a

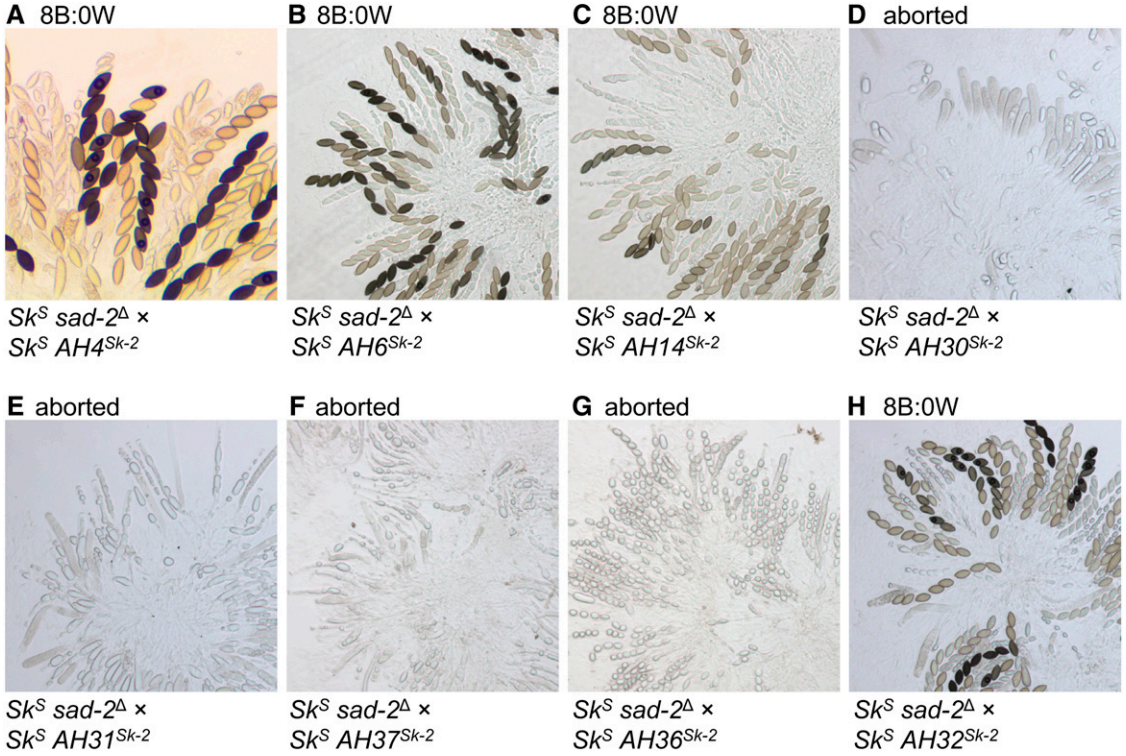

Figure 4 A genetic element within *v5* causes ascus abortion upon its transfer to Sk^S. (A–H) Images depict asci from crosses between Sk^S *sad-2*$^\Delta$ and an Sk^S mating partner. Each Sk^S mating partner carries a different subinterval of *v5*. Crosses are as follows: (A) ISU-3037 × ISU-3224, (B) ISU-3037 × ISU-3228, (C) ISU-3036 × ISU-3243, (D) ISU-3037 × ISU-3656, (E) ISU-3037 × ISU-3658, (F) ISU-3036 × ISU-4269, (G) ISU-3037 × ISU-4271, and (H) ISU-3037 × ISU-3660. B, black; W, white.

protein of at least 102 amino acids (aa). We also present evidence that the stop codon at "position 103" in the *rfk-1* transcript undergoes RNA editing during sexual development. According to standard rules of mRNA translation, the edited *rfk-1* transcript contains the code for a 130-aa protein. Possibilities that the shorter and/or longer RFK-1 protein variants are required for the meiotic drive mechanism are discussed.

Materials and Methods

Strains, media, and crossing conditions

The strains used in this study are listed along with genotype information in Table 1. Vogel's minimal medium (Vogel 1956), with supplements as required, was used to grow and maintain all strains. Hygromycin B and nourseothricin sulfate were used at a working concentration of 200 and 45 μg/ml, respectively. Synthetic crossing medium (pH 6.5) with 1.5% sucrose, as described by Westergaard and Mitchell (1947), was used for crosses. Crosses were unidirectional and performed on a laboratory benchtop at room temperature under ambient lighting (Samarajeewa *et al.* 2014). After fertilization, crosses were allowed to mature for 12–16 days before perithecial dissection in 25 or 50% glycerol. Asci were then examined with a compound microscope (Leica DMBRE) and imaging system. Ascus phenotype designations were based on qualitative observations. More than 90% of the asci from a cross had to display the same phenotype to receive one of the following designations: 8B:0W, 4B:4W, or aborted.

Genetic modification of N. crassa, genotyping, and sequence confirmation

A technique called double-joint polymerase chain reaction (PCR) was used to construct all deletion vectors (Yu *et al.* 2004; Hammond *et al.* 2011). Transgene-insertion vectors were designed to insert transgenes along with a hygromycin resistance cassette (*hph*) next to *his-3* on chromosome I. Construction details for deletion and insertion vectors are provided in Supplemental Material, Tables S1–S5. Transformations of *N. crassa* were performed by electroporation of conidia (Margolin *et al.* 1997). Homokaryons were derived from heterokaryotic transformants with a microconidium isolation technique (Ebbole and Sachs 1990) or by crossing the transformants to a standard laboratory strain (F2-23 or F2-26) to obtain homokaryotic ascospores. Site-directed mutagenesis was performed essentially as described for the QuikChange II Site-Directed Mutagenesis Kit (Revision E.01; Agilent Technologies). Additional details are provided in Table S5. Genotypes were confirmed by PCR assays on genomic DNA isolated from lyophilized (freeze-dried) mycelia with the IBI Scientific's Mini Genomic DNA Kit (Plant/Fungi). Sanger sequencing was used to confirm

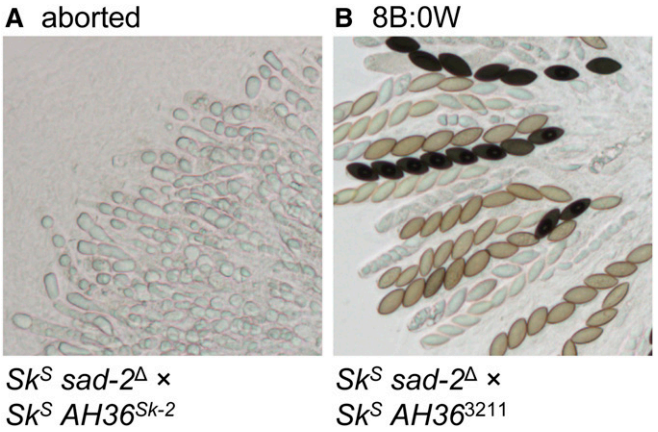

Figure 5 The *AH36* interval from an *rfk-1* mutant does not cause ascus abortion. Images depict asci from crosses between an Sk^S *sad-2*$^\Delta$ strain and an Sk^S strain, carrying either the *AH36* interval from (A) F2-19 (*rfk-1*$^+$) or (B) ISU-3211 (an *rfk-1* mutant). Crosses are as follows: (A) ISU-3037 × ISU-4273 and (B) ISU-3037 × ISU-4275. B, black; W, white.

sequences and/or identify mutations in PCR products and plasmids.

Analysis of RNA sequencing data

Six data sets containing paired-end sequences of poly(A)-enriched RNA from perithecial cultures of *N. intermedia* were downloaded from the Sequence Read Archive (Leinonen *et al.* 2011). The accession numbers for the three Sk^S (FGSC 1767) × *Sk-2* (FGSC 7426) data sets are SRR7700963, SRR7700964, and SRR7700965. Additionally, the accession numbers for the Sk^S (FGSC 1767) × Sk^S (FGSC 1766) data sets are SRR7700966, SRR7700967, and SRR7700968. Sequences from each data set were aligned to the *AH36* interval of *N. intermedia* FGSC 7426 and the actin gene of *N. intermedia* FGSC 1766/8761 with Bowtie 2 (v2.3.4.1) (Langmead and Salzberg 2012). Alignment parameters were as follows: –local, –no-unal, –no-discordant, –no-mixed, –no-overlap, –no-contain, -X 1000. Custom Perl and Python scripts were then used to count each time a position in the reference was covered by a read. Only aligned reads with an edit distance less than four were considered in the coverage calculations. Reads from similar crosses were combined for calculations and charts were generated with Microsoft Excel (data were not normalized among replicate data sets). *N. intermedia AH36* and actin DNA sequences were obtained from the genome sequences of FGSC 7426 and FGSC 1766/8761, respectively (Svedberg *et al.* 2018).

cDNA analysis

For vegetative tissues, total RNA was isolated from 36-hr mycelial cultures grown in liquid Vogel's medium at 32°. For sexual tissues, total RNA was isolated from 6-day-old perithecia from a unidirectional cross between Sk^S (F2-26) and *Sk-2* (P15-53), where Sk^S was used as the female. Vegetative tissues were lyophilized before RNA isolation. In contrast, fresh sexual tissues were directly ground in TRIzol reagent (Invitrogen, Carlsbad, CA) with a mortar and pestle. For both vegetative and sexual total RNA isolations, TRIzol was used at a ratio of 1.5 ml TRIzol per 100 mg of tissue. The remainder of the TRIzol-based RNA isolation procedure was performed according to the manufacturer's recommendations. The RNA pellets from the TRIzol isolation were purified with the PureLink RNA Mini Kit (Invitrogen) by following the manufacturer's instructions for RNA isolation with an on-column DNAse treatment. First-strand cDNA synthesis was then performed with the ProtoScript First Strand cDNA Synthesis Kit (New England Biolabs, Beverly, MA) and the kit's included oligo-d(T) primer. Following first-strand cDNA synthesis, the reaction mixture was diluted with sterile water to a final volume of 50 μl. cDNA fragments were then amplified with standard PCR reactions. Amplified cDNA fragments were purified by agarose gel extraction and analyzed by Sanger sequencing without cloning. Sanger sequencing data and chromatograms were visualized with BioEdit (Hall 1999).

Data availability

All strains and plasmids generated during this study are available upon request. Supplemental material available at Figshare: https://doi.org/10.25386/genetics.7836692.

Results

Deletion of a DNA interval within Sk-2^{INS1} eliminates spore killing

As described in the *Introduction*, we previously mapped *rfk-1* to a 45-kb interval of *Sk-2*. Additionally, this interval was predicted to contain 14 protein-coding genes, two pseudogenes (denoted with an asterisk), an inverted sequence (*Sk-2*^{INV1}), an inversion breakpoint, and an 11-kb insertion (*Sk-2*^{INS1}) (Figure 1B; GenBank: KJ908288.1; Harvey *et al.* 2014). To further refine the location of *rfk-1* within the 45-kb interval, we deleted subintervals *v3*, *v4*, and *v5* (Figure 1B and Table 2). The resulting deletion strains were then crossed to an Sk^S mating partner. While spore killing was functional in both Sk^S × *Sk-2 v3*$^\Delta$ and Sk^S × *Sk-2 v4*$^\Delta$ crosses (asci were 4B:4W; Figure 1, C and D), it was absent in an Sk^S × *Sk-2 v5*$^\Delta$ cross (asci were 8B:0W; Figure 1E). These results suggest that *v5* contains *rfk-1*. To refine the position of *rfk-1* within *v5*, we constructed nine deletion strains (Figure 2, A and B and Table 2) and crossed each one to an Sk^S mating partner. Surprisingly, while deletion of the previously annotated genes and pseudogenes within *Sk-2*^{INS1} had no effect on spore killing (Figure 3, A–D), deletion of the intergenic region between *ncu07838** and *ncu06238* eliminated it (Figure 3, E–I). These results suggest that *rfk-1* is found within the intergenic region between *ncu07838** and *ncu06238*.

An ascus-aborting element exists between ncu07838 and ncu06238*

To determine if a segment of *v5* could induce spore killing when transferred to an Sk^S genetic background, we genetically

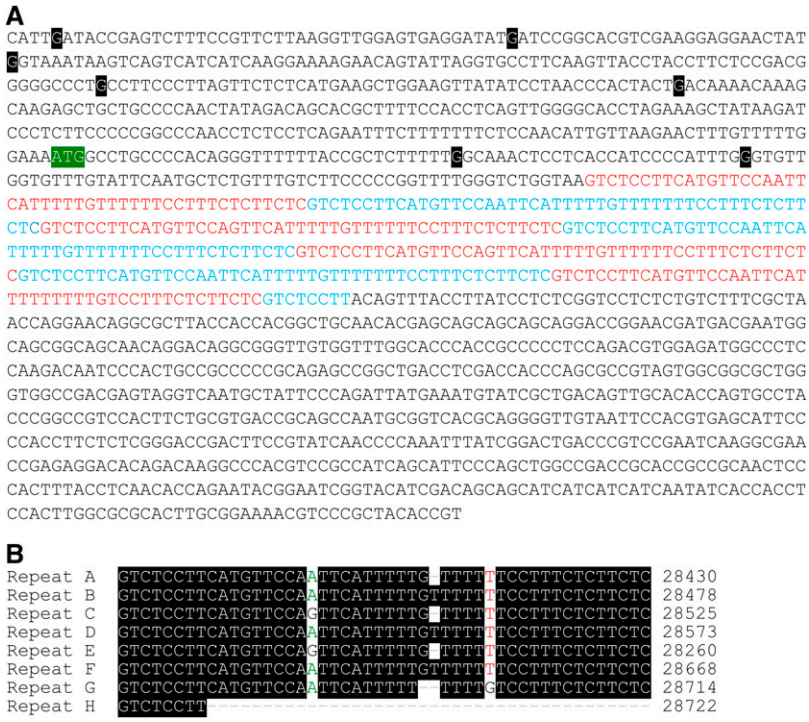

Figure 6 The *AH36* interval from an *rfk-1* mutant contains seven point mutations. (A) The 1481-bp sequence of *AH36*$^{Sk\text{-}2}$ is shown. A region containing 7.17 repeats of a 46–48-bp sequence is highlighted with red font and blue font. The colors alternate with each iteration of the repeated sequence. The sequence of *AH36*^{3211} contains seven G-to-A transition mutations. The position of each mutation is marked by a white character on a black background with the nonmutated base shown. The mutations in *AH36*^{3211} are (from left to right): G27904A, G27945A, G27972A, G28052A, G28104A, G28300A, and G28326A. The putative *rfk-1* start codon is depicted with white characters on a green background. (B) Alignment of the repetitive sequences highlighted in (A).

modified eight *Sk*^{S} strains to carry different *v5* subintervals (Figure 2C and Table 2). However, none of the *v5*-subintervals caused spore killing when crosses were performed between subinterval-carrying strains and a standard *Sk*^{S} mating partner (Figure S1). These results can be explained by the existence of MSUD, a genome defense process that silences unpaired DNA during meiosis (*e.g.*, transgenes that are not found at the same location in the genomes of both parents of a cross; Aramayo and Selker 2013; Hammond 2017). Therefore, to prevent MSUD from silencing the *v5*-subinterval transgenes, we crossed the *v5*-subinterval-carrying strains to an *Sk*^{S} *sad-2*$^{\Delta}$ mating partner [the *sad-2*$^{\Delta}$ allele suppresses MSUD when present in one parent of a cross (Shiu *et al.* 2006)]. In these crosses, four of the *v5* subintervals had no discernable effect on ascus development (*AH4*, *AH6*, *AH14*, and *AH32*), while four others correlated with an ascus abortion phenotype (*AH30*, *AH31*, *AH36*, and *AH37*) (Figure 2C and Figure 4). It seems likely that ascus abortion occurs when a subinterval carries a functional *rfk-1* allele. A traditional 4B:4W ascus phenotype is not possible in these crosses because both parents lack a resistant *rsk* allele. In summary, these experiments demonstrate that *rfk-1* should reside within a subinterval of *v5* that is shared among *AH30*, *AH31*, *AH36*, and *AH37*.

A point mutation disrupts the ascus-aborting ability of AH36$^{Sk\text{-}2}$

AH36 is the shortest (1481 bp) of the four abortion-inducing intervals identified above and is nested within each of them (Figure 2C and Table 2). More specifically, *AH36* is found between positions 27,899 and 29,381 of the previously defined 45-kb *rfk-1* region (GenBank: KJ908288.1 and Table 2). We predicted that the *AH36* interval from ISU-3211 (a genetically defined *rfk-1* mutant strain) would not cause ascus abortion if it were transferred to an *Sk*^{S} strain and analyzed in a cross with an *Sk*^{S} *sad-2*$^{\Delta}$ mating partner. Indeed, comparison of *Sk*^{S} *sad-2*$^{\Delta}$ × *AH36*$^{Sk\text{-}2}$ and *Sk*^{S} *sad-2*$^{\Delta}$ × *AH36*^{3211} crosses indicates that the *AH36* interval from *Sk-2* (called *AH36*$^{Sk\text{-}2}$) causes ascus abortion and that the *AH36* interval from ISU-3211 (called *AH36*^{3211}) does not (Figure 5).

The inability of *AH36*^{3211} to cause ascus abortion suggests that it differs from *AH36*$^{Sk\text{-}2}$ at the sequence level. By sequencing *AH36*^{3211}, we identified seven guanine-to-adenine transition mutations relative to *AH36*$^{Sk\text{-}2}$ (Figure 6A; G27904A, G27945A, G27972A, G28052A, G28104A, G28300A, and G28326A). We then used site-directed mutagenesis to determine which, if any, of these mutations eliminated *AH36*^{3211}'s ability to abort asci. For each mutation, this involved mutating the base in a clone of *AH36*$^{Sk\text{-}2}$, placing the mutated interval (*e.g.*, *AH36*$^{Sk\text{-}2[G27945A]}$) in an *Sk*^{S} strain, and crossing the transgenic strain to an *Sk*^{S} *sad-2*$^{\Delta}$ mating partner. Of the six mutations tested, only G28326A eliminated the ascus-aborting ability of *AH36*$^{Sk\text{-}2}$ (Figure 7).

A start codon for RFK-1

The G28326A mutation is found ~60 bp downstream of a putative start codon at positions 28,264–28,266 (Figure 6A). To test if this "ATG" is the start codon for an RFK-1 protein, we constructed three gene replacement vectors: *v199*, *v214*, and *v221*. Vector *v199* inserts the *N. crassa ccg-1* promoter [*ccg-1*(P)] directly upstream of the ATG (Figure 8, A and B). Vector *v214* is nearly identical to *v199*, except that it changes the ATG to ATGT (*i.e.*, it inserts an extra base and induces a

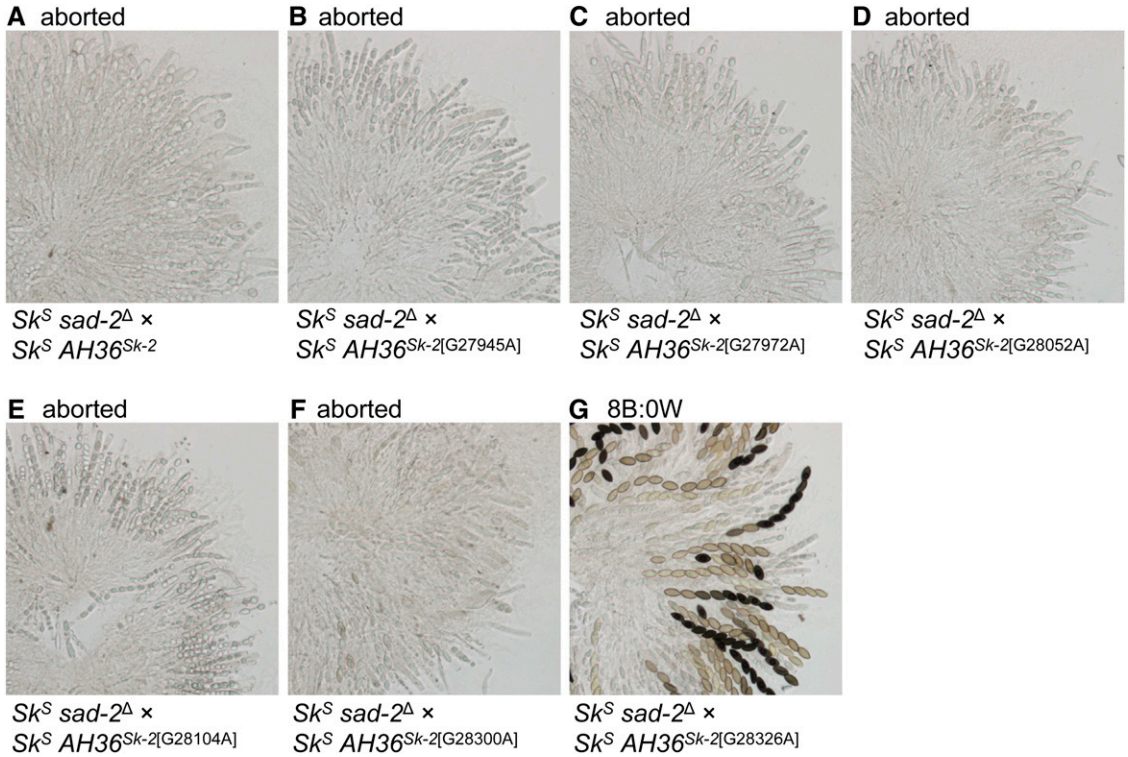

Figure 7 A point mutation within *AH36* eliminates its ability to abort asci. Six of seven point mutations in $AH36^{3211}$ were examined for a potential role in eliminating ascus abortion. Each mutation was placed individually in $AH36^{Sk\text{-}2}$ by site-directed mutagenesis. (A–G) Images depict asci from crosses between an Sk^S *sad-2*$^\Delta$ strain and an Sk^S mating partner carrying $AH36^{Sk\text{-}2}$ or one of its mutated derivatives. Crosses are as follows: (A) ISU-3037 × ISU-4273, (B) ISU-3037 × ISU-4551, (C) ISU-3037 × ISU-4552, (D) ISU-3037 × ISU-4553, (E) ISU-3037 × ISU-4554, (F) ISU-3037 × ISU-4555, and (G) ISU-3037 × ISU-4556. B, black; W, white.

frameshift). Vector *v221* is also nearly identical to *v199*; however, it changes the ATG to TAA (*i.e.*, a stop codon). With these vectors, we found that attaching *ccg-1*(P) to the ATG (with *v199*) has no effect on spore killing (Figure 8, compare C and D) and that changing the ATG to ATGT (with *v214*) or TAA (with *v221*) eliminates spore killing (Figure 8, compare C, E, and F). Together, these results suggest that positions 28,264–28,266 code for a functional *rfk-1* start codon and that *rfk-1* is a protein-coding gene.

The arrangement of rfk-1 within Sk-2 protects it from MSUD

The right border of *Sk-2* is thought to be located at (or very near) position 29,151 (Figure 9A, dotted line; Table 2; Harvey *et al.* 2014). This hypothesis is based on the similarity of DNA sequences found on the centromere-distal side (to "the right") of this position in both *Sk-2* and Sk^S strains. For example, a ClustalW-based alignment (Thompson *et al.* 1994) found that *Sk-2* positions 29,152 through 35,728 are 94.4% identical to the corresponding positions within Sk^S (GenBank: CM002238.1, positions 2,011,073 to 2,017,662). In contrast, the sequences found on the centromere-proximal side ("to the left") of the *Sk-2* right border are completely unrelated between *Sk-2* and Sk^S strains (Figure 9A). Because most of *AH36* is found on the centromere-proximal side of the *Sk-2* border (Figure 9A), most of this interval (including *rfk-1*) should be unpaired during meiosis in Sk^S × *Sk-2* crosses. Assuming *rfk-1* is unpaired during meiosis, how does it avoid silencing by MSUD? While the molecular details of how MSUD detects unpaired DNA are mostly unknown, we considered the possibility that the short distance of *rfk-1* from a "paired" sequence allows it to avoid MSUD (*e.g.*, note that the *ncu06238* genes in *Sk-2* and Sk^S are paired and that *AH36* is located relatively close to these paired genes; Figure 9A). To test this hypothesis, we inserted a hygromycin resistance cassette (*hph*) between *AH36* and the *Sk-2* right border in a standard *Sk-2* strain (Figure 9A). We refer to this particular *hph* transgene as *v140*$^\Delta$::*hph*. The *v140*$^\Delta$::*hph* transgene increased the distance of *rfk-1* from paired sequences by a length of 1391 bp. As a control, we inserted a similar transgene called *v150*$^\Delta$::*hph* at the corresponding location in an Sk^S strain. In agreement with our hypothesis, an Sk^S × *Sk-2 v140*$^\Delta$::*hph* cross lacked signs of spore killing, while spore killing was normal in an Sk^S *v150*$^\Delta$::*hph* × *Sk-2 v140*$^\Delta$::*hph* cross (Figure 9, B and C). These results suggest that if *rfk-1* is located too far from paired DNA, it is detected by MSUD and silenced. As an additional test of this hypothesis (*rfk-1* must be located near paired DNA to avoid MSUD), we analyzed asci from an Sk^S *sad-2*$^\Delta$ × *Sk-2 v140*$^\Delta$::*hph* cross and found spore killing to be normal (Figure 9D). This outcome can be

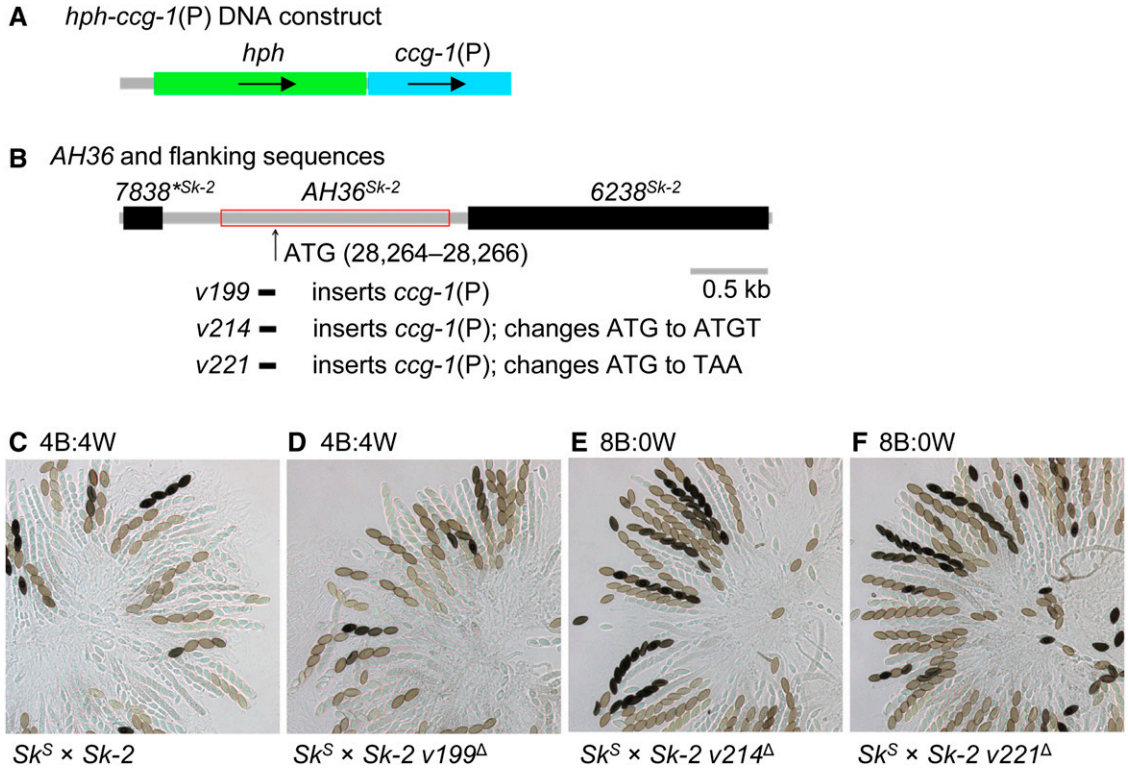

Figure 8 A putative start codon for RFK-1 exists within *AH36*. (A) A DNA construct consisting of *hph* (a hygromycin resistance cassette) and the promoter for the *N. crassa ccg-1* gene was used to make three transformation vectors: *v199*, *v214*, and *v221*. (B) Vector *v199* replaces 133 bp of *AH36* while fusing *ccg-1*(P) to a putative start codon at position 28,264. Vector *v214* and *v221* are nearly identical to *v199*, except that they change the start codon to ATGT and TAA, respectively. (C–F) Crosses were performed to determine the effect of each allele on spore killing. Images depict asci from the following crosses: (C) F2-26 × P15-53, (D) F2-26 × ISU-4557, (E) F2-26 × ISU-4576, and (F) F2-26 × ISU-4584. With respect to the image labels, $v199^{\Delta}$, $v214^{\Delta}$, and $v221^{\Delta}$ are abbreviations of $v199^{\Delta}$::*hph-ccg-1*(P)-ATG, $v214^{\Delta}$::*hph-ccg-1*(P)-ATGT, and $v221^{\Delta}$::*hph-ccg-1*(P)-TAA, respectively. B, black; W, white.

explained by the presence of $sad\text{-}2^{\Delta}$, which suppresses MSUD and makes the distance of *rfk-1* from paired DNA irrelevant to its expression during meiosis.

The rfk-1 gene does not include ncu06238

To confirm that *ncu06238*, the gene to the right of *rfk-1* (as depicted in Figure 9A), is neither part of *rfk-1* nor required for spore killing, we deleted *ncu06238* from both Sk^S and *Sk-2* and then analyzed ascus phenotypes in crosses involving the *ncu06238* deletion strains. Interestingly, an Sk^S $ncu06238^{\Delta}$ × Sk^S cross produced asci with varying numbers of fully developed ascospores (Figure 10A), suggesting that *ncu06238* deletion strains have defects in ascosporogenesis that are independent of *Sk-2* and spore killing. As a result, we could not use ascus phenotype to determine if spore killing is functional in an Sk^S $ncu06238^{\Delta}$ × *Sk-2* $ncu06238^{\Delta}$ cross, where asci also produce varying numbers of ascospores (Figure 10B). To overcome this obstacle, we used PCR to check genotypes of progeny from an Sk^S $ncu06238^{\Delta}$ × *Sk-2* $ncu06238^{\Delta}$ cross. If *Sk-2*-based spore killing occurred in this cross, most progeny would have an *Sk-2* genotype. Indeed, we found that 34 of 35 progeny had the *Sk-2* genotype (Figure S2), indicating that *Sk-2*-based meiotic drive functions normally in the absence of *ncu06238*. These results strongly suggest that the *rfk-1* gene does not overlap or include positions occupied by *ncu06238*.

Replacement of $AH36^{3211}$ with $AH36^{Sk\text{-}2}$ restores spore killing to an rfk-1 mutant

The *rfk-1* mutant strain ISU-3211 carries seven mutations within its *AH36* interval (Figure 6A and Figure 11A). Although we have already shown that introduction of the G28326A mutation carried by $AH36^{3211}$ into $AH36^{Sk\text{-}2}$ eliminates $AH36^{Sk\text{-}2}$'s ability to abort asci (Figure 7G), we have not directly shown that one or more of the mutations within $AH36^{3211}$ causes ISU-3211's loss-of-spore-killing phenotype. To address this shortcoming, we replaced $AH36^{3211}$ in a descendant of ISU-3211 (ISU-3222) with $AH36^{Sk\text{-}2}$::*hph* (Figure 11A) and crossed it to Sk^S and Sk^S $v150^{\Delta}$::*hph* mating partners. As expected, we found that replacing $AH36^{3211}$ with $AH36^{Sk\text{-}2}$::*hph* restored spore killing as long as the *hph* marker was "paired" during meiosis (Figure 11, B–G). These results demonstrate that mutations within the *AH36* interval are solely responsible for the loss of spore killing in ISU-3211 and its *rfk-1* descendants.

rfk-1 is transcribed

To learn more about *rfk-1*'s gene structure, we analyzed RNA sequencing data sets of poly(A)-enriched total RNA from

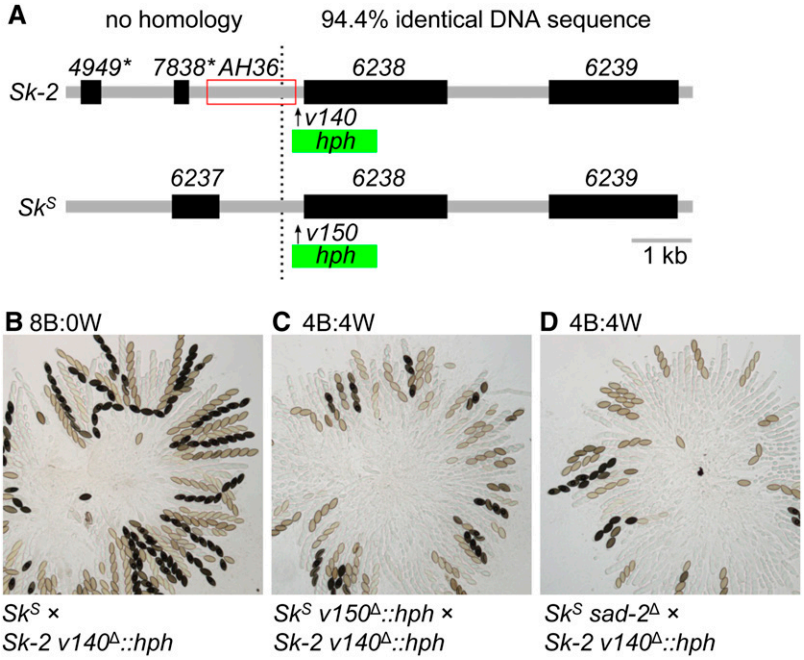

Figure 9 The native arrangement of *rfk-1* protects it from meiotic silencing by unpaired DNA. (A) Interval *AH36* spans the right border of *Sk-2* (marked by a black dotted line). An *hph* marker was placed immediately to the right of *AH36* in an *Sk-2* strain (with vector *v140*) to create the *v140*$^{\Delta}$::*hph* allele. An *hph* marker was also placed at the corresponding location in an *Sk*^{S} strain (with vector *v150*) to create the *v150*$^{\Delta}$::*hph* allele. (B–D) Crosses were performed to determine the effect of each allele on spore killing. Images depict asci from the following crosses: (B) F2-23 × ISU-4344, (C) ISU-4348 × ISU-4344, and (D) ISU-3036 × ISU-4344. B, black; *hph*, hygromycin resistance cassette; W, white.

perithecial cultures of *N. intermedia Sk*^{S} × *Sk-2* and *Sk*^{S} × *Sk*^{S} crosses (Svedberg *et al.* 2018). The *AH36* intervals in *N. crassa* F2-19 (referred to as *AH36*$^{Sk\text{-}2}$) and *N. intermedia* FGSC 7426 (*AH36*^{7426}) are nearly identical, except for one single-nucleotide polymorphism and a 48-bp insertion/deletion (Figure S3). As expected, while relatively few reads from *Sk*^{S} × *Sk*^{S} perithecia align to *AH36*^{7426}, hundreds of reads from the *Sk*^{S} × *Sk-2* perithecia do align to this sequence (Figure 12A). In contrast, *Sk*^{S} × *Sk*^{S} and *Sk*^{S} × *Sk-2* perithecia contain similar levels of reads that align to the actin gene (Figure 12B). By assuming that the majority of *AH36*^{7426}-aligning reads from *Sk*^{S} × *Sk-2* perithecia are derived from *rfk-1* transcripts, we can predict that the *rfk-1* gene contains four exons and three introns (Figure 12A and Figure S3). Furthermore, by using the ATG at positions 28,264–28,266 (Figure 8) as the putative *rfk-1* translational start codon, we can detect a translational stop codon upstream of the second intron ("TAG"; Figure 12A and Figure S4). This stop codon should terminate translation after production of a 102-aa RFK-1 protein. However, if the stop codon were to undergo RNA editing (discussed in more detail below), a different translational stop codon ("TAA"; Figure 12A and Figure S4) should terminate translation after production of a 130-aa RFK-1 protein.

The rfk-1 transcript undergoes RNA editing during sexual development

During the aforementioned analysis of RNA sequencing reads from perithecial cultures of *N. intermedia Sk*^{S} × *Sk-2* crosses, we noticed that the majority of reads mapping to the putative "TAG" stop codon located upstream of intron 2 (Figure 12A and Figure S4) contained evidence of RNA editing. More specifically, the codon appears to be edited from UAG to UGG (or more likely U-Inosine-G, see *Discussion* and Figure S5). In light of this discovery, we amplified partial *rfk-1* cDNA fragments from *N. crassa Sk-2* total RNA extracts and directly analyzed the cDNA fragments by Sanger sequencing (without subcloning). We found that *rfk-1* cDNA fragments from vegetative tissue showed no evidence of RNA editing, while cDNA fragments from sexual tissue contained the expected UAG to UGG edit (Figure 13). These data demonstrate that the early UAG stop codon within *rfk-1* transcripts undergoes RNA editing during sexual development.

The rfk-1 complementation group possesses codon-altering mutations

We previously identified six *rfk-1* mutants, ISU-3211 through ISU-3216, and all strains were determined to be *rfk-1* mutants by complementation group analysis (Harvey *et al.* 2014). If our *rfk-1* gene model is accurate, each strain should carry a mutation that alters *rfk-1*'s transcriptional or coding potential in a manner that is consistent with our model. Indeed, the sequencing of *rfk-1* alleles in ISU-3211 through ISU-3216 identified putative codon-altering mutations in each strain (Figure 14A). For example, ISU-3211 contains the G28326A mutation (examined by site-directed mutagenesis in Figure 7). This mutation changes the 21st *rfk-1* codon to a stop codon (nonsense mutation). ISU-3212 carries a single-base insertion that causes a frameshift after the eighth *rfk-1* codon. ISU-3213 possesses a G28348A mutation, which changes the amino acid specified by the 29th codon from alanine to threonine. With respect to the remaining three strains—ISU-3214, ISU-3215, and ISU-3216—they all contain *rfk-1* sequences that are identical to that of ISU-3211, suggesting that all four were derived from the same mutagenized conidium (via fertilization of an *Sk*^{S} protoperithecium; Harvey *et al.* 2014). In summary, all known genetically defined *rfk-1* mutants carry mutations that alter the predicted coding

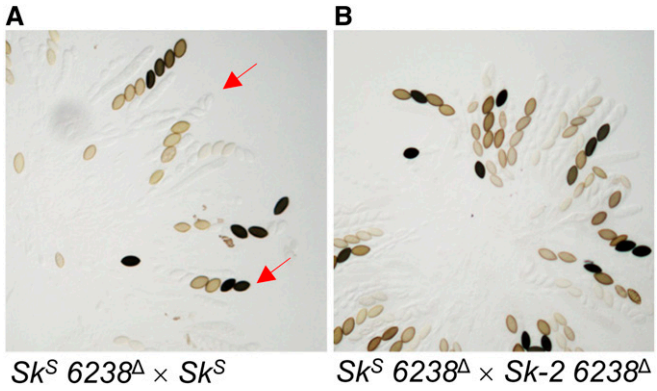

Figure 10 The *ncu06238* gene is not required for spore killing. (A) Asci from a cross between two Sk^S strains (ISU-4559 × P8-43), where one of the strains has had its *ncu06238* coding sequence deleted. While some normal asci are detected, many asci are abnormal and some mimic the Spore killer phenotype (red arrows). (B) Asci from a cross between an Sk^S strain and an *Sk-2* strain (ISU-4559 × ISU-4561), where both strains have had their *ncu06238* coding sequence deleted. Nearly all viable progeny isolated from this cross have the *Sk-2* genotype (34 out of 35; Figure S2).

region of *rfk-1* and support our current model of *rfk-1* gene structure.

RFK-1 is related to NCU07086

To investigate the origin of *rfk-1*, we downloaded a list of predicted *N. crassa* proteins from the National Center for Biotechnology Information (NCBI)'s Genome Database (accession number GCA_000182925.2) and performed a BLASTP search (Basic Local Alignment Search Tool - Protein; Camacho *et al.* 2009) with the 130-aa RFK-1 sequence as query (Figure S4). We found that the most significant match (Expect = 2e−5) to RFK-1 is a hypothetical 362-aa protein called NCU07086 (GenBank: EAA31115.1). NCU07086 is encoded by the *ncu07086* gene on *N. crassa* chromosome VI, and it is predicted to contain four introns (Figure 14B, I1 through I4; NCBI Gene ID, 3876500). A search of NCBI's conserved domain database (CDD v3.16; Marchler-Bauer *et al.* 2015) with the predicted sequence of NCU07086 identified a region with a low-scoring match to the AtpF superfamily (Expect = 2.23e−3; Figure 12B). The similarity between RFK-1 and NCU07086 appears to be reserved to the N-terminal ends of each protein. Specifically, the first 39 amino acids of RFK-1 are highly similar to those of NCU07086 (Figure 14C). Furthermore, it appears that a 47-bp sequence within *ncu07086*'s first intron (Figure 14D) expanded to become the 46–48-bp repeated element within *rfk-1*'s first intron (Figure 6, A and B, and Figure 14D). In summary, these findings suggest that *rfk-1* evolved from a partial duplication of the *ncu07086* gene.

Discussion

The mechanism used by the *Neurospora* Spore killers to achieve biased transmission is believed to involve a resistance protein and a killer protein. In a previous work, we isolated six *rfk* mutants (ISU-3211 through ISU-3216) and provided evidence that each is mutated at the same locus, subsequently named *rfk-1* (Harvey *et al.* 2014). The *rfk-1* locus in ISU-3211 was mapped to a 45-kb region of *Sk-2*. We began this study with the goal of identifying *rfk-1*. At first, we intended to use three-point crossing assays to further refine the position of *rfk-1* within the 45-kb region. These assays were to be performed with *hph* markers inserted between genes *ncu06192* and *ncu06191* (with vector *v3*) and between genes *ncu06239* and *ncu06240* (with vector *v4*); therefore, deletion vectors *v3* and *v4* were designed to delete relatively small intervals from the *rfk-1* region (Table 2) and, as such, they were not expected to influence spore killing. In agreement with our predictions, deletion of intervals *v3* and *v4* had no effect on spore killing (Figure 1, C and D). In contrast, *v5* was designed to delete a 10,718-bp interval spanning most of the $Sk\text{-}2^{INS1}$ sequence, with the goal of deleting *rfk-1* should it exist within the interval (Table 2). Fortunately, deletion of *v5* was fruitful and its removal from *Sk-2* eliminated *Sk-2*'s ability to kill ascospores (Figure 1E). We were thus able to focus our efforts on deleting subintervals of *v5*, which allowed us to pinpoint *rfk-1* to the intergenic region between *ncu07238** and *ncu06238* (Figure 2 and Figure 3).

We also tested various subintervals of *v5* for the presence of *rfk-1* by transferring them to an Sk^S strain and crossing them to an Sk^S $sad\text{-}2^{\Delta}$ mating partner (Figure 4). For this assay to yield positive results, *rfk-1* must be sufficient for spore killing. Indeed, we found this to be the case when we identified four intervals (*AH30*, *AH31*, *AH36*, and *AH37*) that triggered ascus abortion when transferred to an Sk^S genetic background. These four intervals all have the 1481 bp of *AH36* in common, and the ascus abortion phenotype associated with each interval is likely due to the presence of *rfk-1* without a compatible resistance gene. For example, the KN model holds that the resistance protein (RSK) and the killer are both active during early stages of meiosis (Hammond *et al.* 2012). Lack of a resistant version of RSK, along with expression of the killer, appears to cause asci to abort meiosis before ascospore delimitation. This phenomenon explains the abortion phenotypes of *AH30*, *AH31*, and *AH37*. However, for succinctness, we also refer to the phenotype associated with *AH36* as ascus abortion, although it may be more accurate to refer to it as a "bubble" phenotype (see Figure 4G). The bubble phenotype was originally described by Raju *et al.* (1987), and it is thought to arise when asci and/or ascospores abort shortly after ascospore delimitation. Therefore, an explanation for the existence of the two phenotypic classes (clear ascus abortion *vs.* bubble phenotype) is that ascus development progresses a bit further with *AH36* than it does with *AH30*, *AH31*, and *AH37*. In turn, one could speculate that *rfk-1* expression is lower from *AH36* than it is from *AH30*, *AH31*, and *AH37*, because *AH36* is the shortest of the abortion-inducing intervals and may lack some of the regulatory sequences needed for full expression of *rfk-1*.

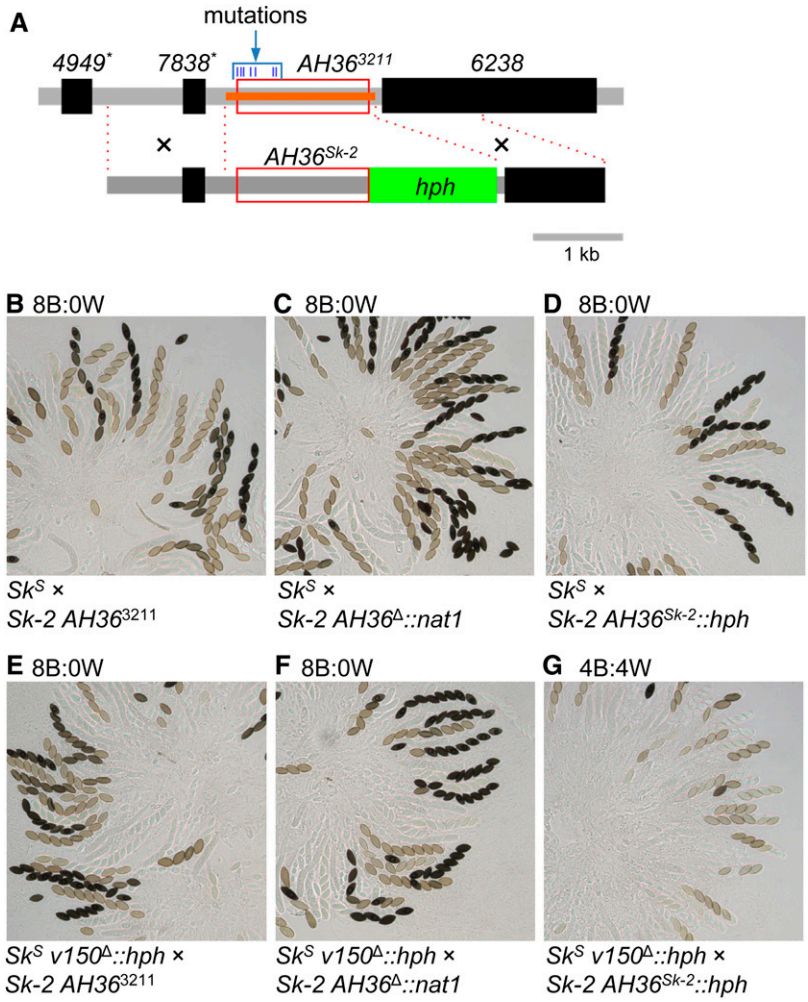

Figure 11 Replacement of *AH36*^{3211} with *AH36*$^{Sk\text{-}2}$ restores spore killing to an *rfk-1* mutant. (A) Strain ISU-4562 was constructed by replacing *AH36*^{3211} in ISU-3222 (upper diagram, red box) with *nat1* (using vector *v160*, with deleted positions indicated with an orange bar; ISU-3222 is a descendant of ISU-3211). Strain ISU-4563 was then constructed by replacing *AH36*$^{\Delta}$::*nat1* in ISU-4562 with *AH36*$^{Sk\text{-}2}$::*hph* (lower diagram, red box and green rectangle). The locations of the two recombination flanks used to replace *AH36*$^{\Delta}$::*nat1* with *AH36*$^{Sk\text{-}2}$::*hph* are indicated with black crosses and red dotted lines. (B–D) Asci are from crosses between F2-23 and (B) ISU-3222, (C) ISU-4562, and (D) ISU-4563. (E–G) Asci are from crosses between ISU-4348 and (E) ISU-3222, (F) ISU-4562, and (G) ISU-4563. See Figure 9 for a description of the *v150*$^{\Delta}$::*hph* allele. B, black; *hph*, hygromycin resistance cassette; W, white.

In this study, we have provided evidence that the critical *rfk-1* coding region is found between a start codon beginning at position 28,264 and either a stop codon ending at position 28,968 or a stop codon ending at position 29,106. For example, (1) a putative nonsense mutation at position 28,326 disrupts the ascus-aborting ability of interval *AH36* (Figure 6A, Figure 7G, and Figure 14A); (2) spore killing functions when a nonnative promoter is attached to the putative *rfk-1* start codon at position 28,264 (Figure 8, B and D); (3) spore killing fails when the putative *rfk-1* reading frame is shifted by one position by the insertion of a single base immediately after the putative start codon (Figure 8, B and E); and (4) spore killing fails when the putative *rfk-1* start codon is changed to a stop codon (Figure 8, B and F). Additionally, all six of the known *rfk-1* mutants carry codon-altering mutations that are consistent with our proposed *rfk-1* gene model (Figure 14A). Furthermore, although we have not identified the transcript cleavage site or the location at which the poly(A) tail is added, we have shown that the gene immediately downstream of *rfk-1* (*ncu06238*) is not required for *rfk-1* function (Figure 10B and Figure S2) and we have detected *rfk-1* cDNAs using reverse transcription reactions primed with an oligo-d(T) primer (Figure 13B). In summary, our data strongly suggest *rfk-1* to be a protein-coding gene with four exons and three introns.

Adenosine-to-inosine (A-to-I) RNA editing was recently discovered in two Sordariomycete fungi: *Fusarium graminearum* and *N. crassa* (Liu *et al.* 2016, 2017). Interestingly, while the enzymes directing A-to-I edits of Soradriomycete RNAs are unknown, the process appears to be specific to the sexual cycle (Liu *et al.* 2016, 2017). While modeling *rfk-1* gene structure with RNA sequencing data, we noticed that the sequences of most of the reads that aligned to the first *rfk-1* stop codon (codon 103) contained mutations relative to the reference sequence and that these mutations (which appear as a "G" in sequencing data) are consistent with A-to-I editing events (Figure S5). We confirmed this finding by amplifying and sequencing *rfk-1*-specific cDNA fragments (Figure 13). Interestingly, and consistent with the presumed sexual phase-specific nature of A-to-I RNA editing in *Neurospora* (Liu *et al.* 2017), *rfk-1* editing was detected in sexual RNA but not vegetative RNA. This raises the possibility that the RNA edit allows *rfk-1* to encode protein variants with different functions, one for the vegetative phase and one for the sexual phase. Although the mechanism of A-to-I editing in fungi is unknown, edited bases are often found at the end of hairpin

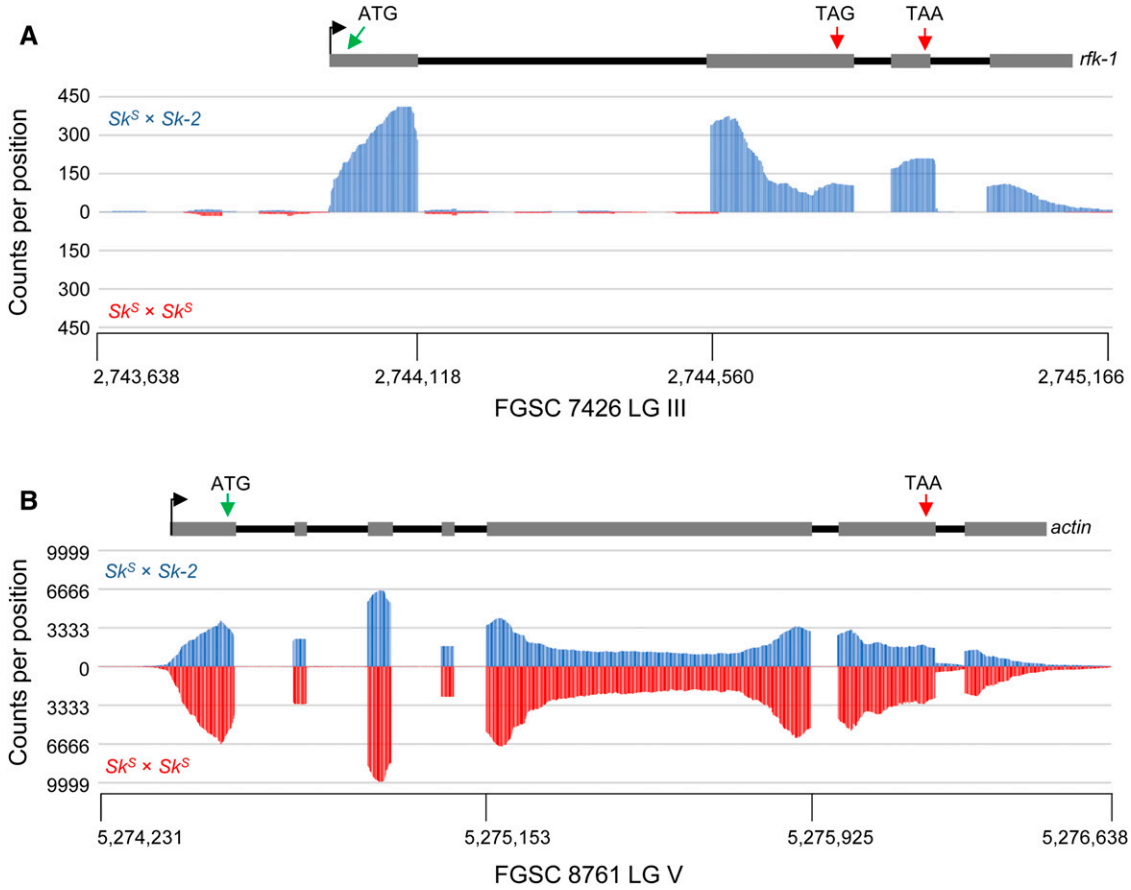

Figure 12 *rfk-1* is transcribed in cultures undergoing sexual reproduction. (A) Sequences of Sk^S × *Sk-2* poly(A)-enriched RNA (top, FGSC 1767 × FGSC 7426) and Sk^S × Sk^S poly(A)-enriched RNA (bottom, FGSC 1767 × FGSC 1766) were aligned to $AH36^{7426}$. The *y*-axis values indicate the number of times each position within $AH36^{7426}$ is found in an aligned RNA sequence. The *x*-axis values indicate the position of each base within $AH36^{7426}$ with respect to chromosome III of *N. intermedia* FGSC 7426. These data suggest that *rfk-1* is transcribed in Sk^S × *Sk-2* perithecial cultures and that *rfk-1* RNA is specific to Sk^S × *Sk-2* crosses. A model of *rfk-1* gene structure is shown above the chart. (B) Sequences of Sk^S × *Sk-2* (top, FGSC 1767 × FGSC 7426) and Sk^S × Sk^S (bottom, FGSC 1767 × FGSC 1766) poly(A)-enriched RNA were aligned to *actin*. In contrast to the $AH36^{7426}$ alignment data, RNA sequences from both Sk^S × *Sk-2* and Sk^S × Sk^S crosses similarly align to *actin* with respect to number and pattern. The *x*-axis values are for the *actin* locus on chromosome V of FGSC 1766.

loops (Liu *et al.* 2017). Accordingly, we found that the edited *rfk-1* stop codon is predicted to exist within the loop of a hairpin with a nearly perfect 18-bp stem region (Figure S6). Overall, the discovery of *rfk-1* transcript editing has fascinating implications for RFK-1 function. For example, it is tempting to speculate that only the edited RNA produces a killer protein and that editing is timed to mitigate potential fitness costs associated with inopportune expression of a functional killer.

While the work presented here represents a significant step toward understanding the mechanism of *Sk-2*-based spore killing, many questions remain unanswered. For example, although it appears that *rfk-1* evolved from *ncu07086*, the function of NCU07086 is unknown. NCU07086 contains a region with slight homology to the AtpF superfamily (Figure 14B). Interestingly, the *atpF* gene in *Escherichia coli* (also known as *uncF*; NCBI Gene ID 948247) encodes subunit b of the F-type ATP synthase complex (Walker *et al.* 1984; Dunn 1992; McLachlin and Dunn 1997; Revington *et al.* 1999). This hints that RFK-1 could mediate spore killing by targeting eukaryotic F-type ATP synthases, which are associated with mitochondrial membranes in eukaryotes (Stewart *et al.* 2014). However, NCU07086 in *N. crassa* has not been investigated, and a much more likely candidate for the b subunit of *N. crassa*'s F-type ATP synthase is found in NCU00502 (Kyoto Encyclopedia of Genes and Genomes oxidative phosphorylation pathway: ncr00190, release 87.0, Kanehisa and Goto 2000; Kanehisa *et al.* 2016). Therefore, at this point in time, a role for RFK-1 in disrupting mitochondrial function as part of the spore-killing process is purely speculative.

Although the primary goal of this work was to identify *rfk-1*, the identity of which has been of interest to meiotic drive researchers since the discovery of *Sk-2* nearly four decades ago, we unexpectedly discovered the strongest evidence to date that genomes in some, if not all, lineages of eukaryotic organisms possess elaborate defense processes to protect themselves from complex meiotic drive elements. With respect to *Neurospora* genomes, this defense process appears

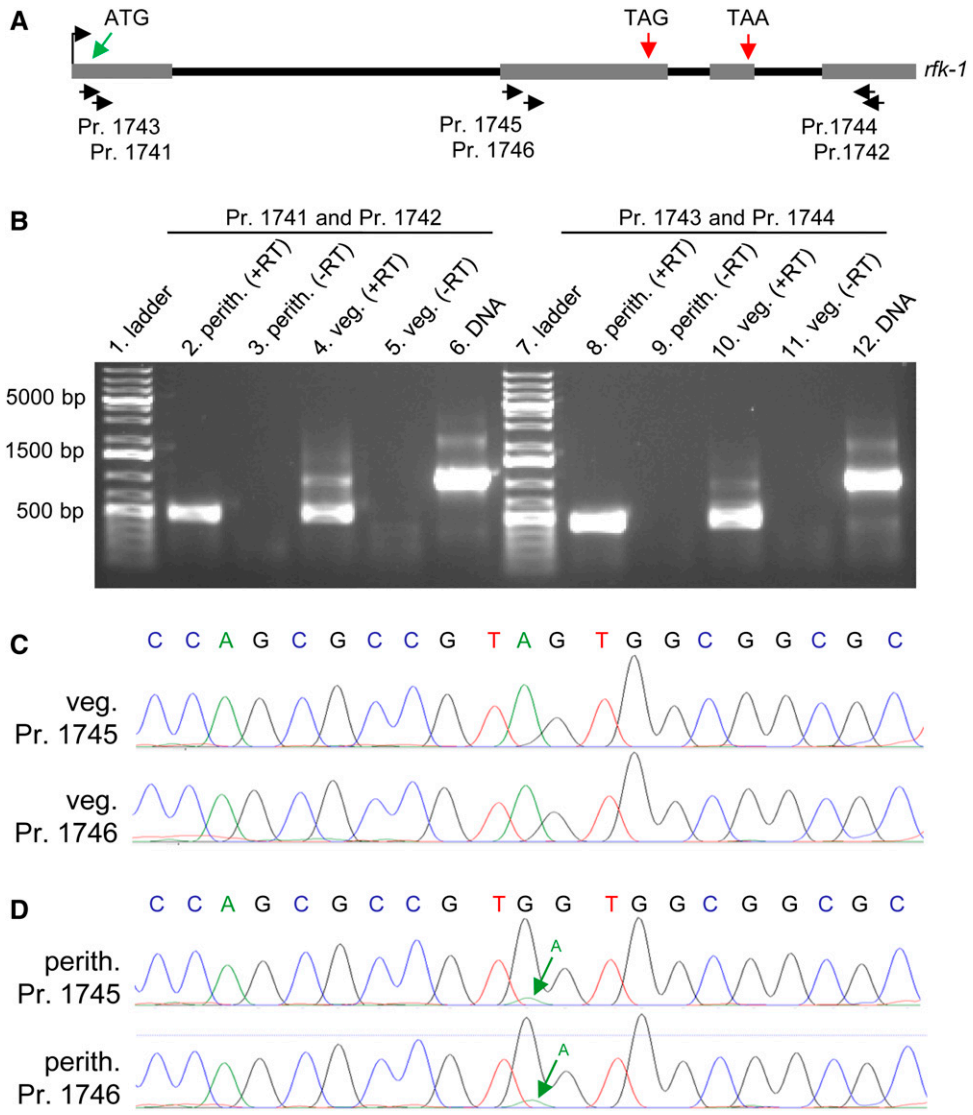

Figure 13 The *rfk-1* mRNA undergoes RNA editing in perithecial tissue. (A) The transcriptional start site (bent arrow), four exons (gray rectangles), and three introns (black lines) of the *rfk-1* gene model are depicted in a diagram. The approximate binding sites of six PCR primers (1741 through 1746) within *rfk-1* are indicated. (B) RT-PCR analysis was performed on total RNA samples isolated from 6-day-old perithecia of an Sk^S (F2-26) × *Sk-2* (P15-53) cross and from *Sk-2* (P15-53) mycelia (36 hr liquid culture). First-strand synthesis was performed with an oligo-dT primer plus reverse transcriptase (+RT). The absence of contaminating DNA was confirmed by leaving reverse transcriptase out of some reactions (−RT). PCR was performed with primers 1741 and 1742 (left) or primers 1743 and 1744 (right), using first-strand cDNA or *Sk-2* (P15-53) genomic DNA as template. RT-PCR products were then analyzed by standard agarose gel electrophoresis and visualized with ethidium bromide staining. (C and D) The sequences of the bases surrounding *rfk-1* codon 103 [the "TAG" in (A)] within the ~500-bp cDNA fragments depicted in panel B's lane 4 and lane 8 were determined directly by Sanger sequencing (without subcloning). (C) Chromatograms from sequencing of the ~500-bp product from panel B's lane 4 with primer 1745 or 1746. No editing of codon 103 (TAG) is detected in the chromatograms. (D) Chromatograms from sequencing of the ~500-bp product from panel B's lane 8 with primer 1745 or 1746. The green arrow points to a small peak whose presence in the chromatograms suggests that a fraction of the cDNA population contains the original A, instead of the edited G, at this position. Perith., perithecia; Pr., primer; veg., vegetative.

to be MSUD. The first hint that MSUD defends *Neurospora* genomes from meiotic drive appeared in 2007, when it was discovered that *Sk-2* and *Sk-3* can suppress certain instances of MSUD (Raju *et al.* 2007). Next, in 2012, it was found that the position of *rsk* within *Sk-2* allows it to pair with *rsk* in the Sk^S genome during *Sk-2* × Sk^S crosses (Hammond *et al.* 2012). If *rsk* is not paired during these crosses (*e.g.*, if it is deleted from the Sk^S mating partner), *rsk* is silenced by MSUD and the entire ascus is killed by the killer protein, which we now know to be RFK-1. In the work presented here, we found that the specific location of *rfk-1* next to the right border of *Sk-2* is critical to the success of meiotic drive because it allows *rfk-1* to escape inactivation by MSUD. Unlike *rsk*, *rfk-1* is only found in *Sk-2* strains and it cannot be paired in *Sk-2* × Sk^S crosses. It appears that the evolutionary forces that drove *Sk-2* into existence found a way to circumvent this problem (*i.e.*, the lack of an *rfk-1* pairing partner in Sk^S strains) by positioning *rfk-1* close to sequences that are paired during meiosis (*i.e.*, close to *ncu06238*, see Figure 9A). While previous work has clearly demonstrated the ability of MSUD to target an unpaired transposon for silencing (and thus defend the genome from transposition events during meiosis; Wang *et al.* 2015), our findings add to accumulating evidence that MSUD also antagonizes the evolution of meiotic drive elements by placing significant constraints on the arrangement of critical genes within these elements. In the future, it will be interesting to learn which process (defense against transposable elements or defense against meiotic drive elements) better explains why MSUD has evolved, and why it has been maintained, in various fungal lineages.

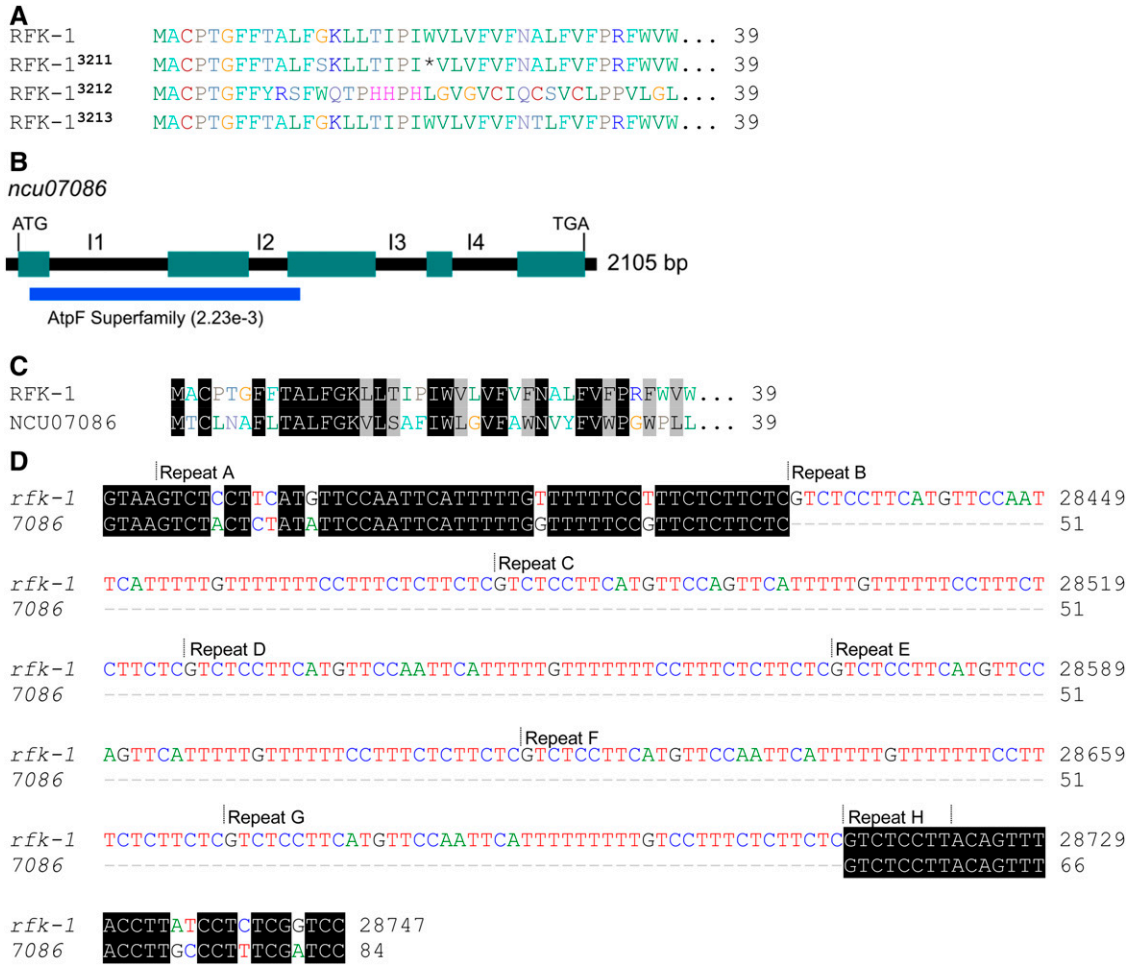

Figure 14 RFK-1 is related to NCU07086. (A) All known *rfk-1* mutations alter the predicted amino acid sequence of RFK-1. (B) A coding region of 2105 bp is predicted for gene *ncu07086* (from start codon to stop codon, including introns). Predicted introns are labeled I1 through I4. An AtpF superfamily domain (National Center for Biotechnology Information conserved domain database, accession number cl28522) can be identified within the N-terminal end of the NCU07086 protein sequence. (C) The first 39 amino acids of RFK-1 and NCU07086 are similar. (D) The repetitive sequence identified within *AH36* (see Figure 6) appears to have originated from within the first intron of *ncu07086*. To highlight the expansion of the 46–48 repeat within the first intron of *rfk-1* relative to the first intron of *ncu07086*, the 5′ end (84 bases) of *ncu07086*'s intron 1 was manually aligned to the 5′ end (368 bases) of *rfk-1*'s intron 1.

Acknowledgments

We thank members of the Brown, Hammond, Johannesson, and Shiu laboratories for their assistance with various technical aspects of this work; and the Fungal Genetics Stock Center, whose preservation and distribution of *Neurospora* isolates helped make this work possible (McCluskey *et al.* 2010). We acknowledge use of materials generated by grant P01 GM-068087 "Functional analysis of a model filamentous fungus." We dedicate this paper to David Perkins, Namboori Raju, Barbara Turner, and others for their pioneering work on the *Neurospora* Spore killers. This project was supported by a grant from the National Science Foundation (NSF) (MCB# 1615626) (T.M.H.). P.K.T.S. was supported by the NSF (MCB# 1715534) and the University of Missouri Research Board and Research Council. H.J. was supported by a European Research Council grant (under the program H2020, ERC-2014-CoG, project 648143) and the Swedish Research Council. Mention of trade names or commercial products in this article is solely for the purpose of providing specific information and does not imply recommendation or endorsement by the U.S. Department of Agriculture (USDA). The USDA is an equal opportunity provider and employer.

Literature Cited

Aramayo, R., and E. U. Selker, 2013 *Neurospora crassa*, a model system for epigenetics research. Cold Spring Harb. Perspect. Biol. 5: a017921. https://doi.org/10.1101/cshperspect.a017921

Bravo Núñez, M. A., N. L. Nuckolls, and S. E. Zanders, 2018 Genetic villains: killer meiotic drivers. Trends Genet. 34: 424–433. https://doi.org/10.1016/j.tig.2018.02.003

Burt, A., and R. Trivers, 2008 *Genes in Conflict: The Biology of Selfish Genetic Elements*. Harvard University Press, Cambridge, MA.

Camacho, C., G. Coulouris, V. Avagyan, N. Ma, J. Papadopoulos *et al.*, 2009 BLAST+: architecture and applications. BMC Bioinformatics 10: 421. https://doi.org/10.1186/1471-2105-10-421

Campbell, J. L., and B. C. Turner, 1987 Recombination block in the Spore killer region of *Neurospora*. Genome 29: 129–135. https://doi.org/10.1139/g87-022

Dalstra, H. J. P., K. Swart, A. J. M. Debets, S. J. Saupe, and R. F. Hoekstra, 2003 Sexual transmission of the [Het-S] prion leads to meiotic drive in *Podospora anserina*. Proc. Natl. Acad. Sci. USA 100: 6616–6621. https://doi.org/10.1073/pnas.1030058100

Davis, R. H., 2000 *Neurospora: Contributions of a Model Organism*. Oxford University Press, New York.

Dunn, S. D., 1992 The polar domain of the b subunit of *Escherichia coli* F_1F_0-ATPase forms an elongated dimer that interacts with the F_1 sector. J. Biol. Chem. 267: 7630–7636.

Ebbole, D., and M. Sachs, 1990 A rapid and simple method for isolation of *Neurospora crassa* homokaryons using microconidia. Fungal Genet. Newsl. 37: 17–18.

Grognet, P., H. Lalucque, F. Malagnac, and P. Silar, 2014 Genes that bias Mendelian segregation. PLoS Genet. 10: e1004387. https://doi.org/10.1371/journal.pgen.1004387

Hall, T. A., 1999 BioEdit: a user-friendly biological sequence alignment editor and analysis program for Windows 95/98/NT. Nucleic Acids Symp. Ser. 41: 95–98.

Hammond, T. M., 2017 Sixteen years of meiotic silencing by unpaired DNA. Adv. Genet. 97: 1–42. https://doi.org/10.1016/bs.adgen.2016.11.001

Hammond, T. M., H. Xiao, D. G. Rehard, E. C. Boone, T. D. Perdue *et al.*, 2011 Fluorescent and bimolecular-fluorescent protein tagging of genes at their native loci in *Neurospora crassa* using specialized double-joint PCR plasmids. Fungal Genet. Biol. 48: 866–873. https://doi.org/10.1016/j.fgb.2011.05.002

Hammond, T. M., D. G. Rehard, H. Xiao, and P. K. T. Shiu, 2012 Molecular dissection of *Neurospora* Spore killer meiotic drive elements. Proc. Natl. Acad. Sci. USA 109: 12093–12098. https://doi.org/10.1073/pnas.1203267109

Harvey, A. M., D. G. Rehard, K. M. Groskreutz, D. R. Kuntz, K. J. Sharp *et al.*, 2014 A critical component of meiotic drive in *Neurospora* is located near a chromosome rearrangement. Genetics 197: 1165–1174. https://doi.org/10.1534/genetics.114.167007

Hu, W., Z. D. Jiang, F. Suo, J. X. Zheng, W. Z. He *et al.*, 2017 A large gene family in fission yeast encodes spore killers that subvert Mendel's law. Eng. Life Sci. 6: e26057.

Kanehisa, M., and S. Goto, 2000 KEGG: kyoto encyclopedia of genes and genomes. Nucleic Acids Res. 28: 27–30. https://doi.org/10.1093/nar/28.1.27

Kanehisa, M., Y. Sato, M. Kawashima, M. Furumichi, and M. Tanabe, 2016 KEGG as a reference resource for gene and protein annotation. Nucleic Acids Res. 44: D457–D462. https://doi.org/10.1093/nar/gkv1070

Kanizay, L. B., T. Pyhäjärvi, E. G. Lowry, M. B. Hufford, D. G. Peterson *et al.*, 2013 Diversity and abundance of the abnormal chromosome 10 meiotic drive complex in *Zea mays*. Heredity 110: 570–577. https://doi.org/10.1038/hdy.2013.2

Langmead, B., and S. L. Salzberg, 2012 Fast gapped-read alignment with Bowtie 2. Nat. Methods 9: 357–359. https://doi.org/10.1038/nmeth.1923

Larracuente, A. M., and D. C. Presgraves, 2012 The selfish *Segregation Distorter* gene complex of *Drosophila melanogaster*. Genetics 192: 33–53. https://doi.org/10.1534/genetics.112.141390

Leinonen, R., H. Sugawara, and M. Shumway International Nucleotide Sequence Database Collaboration 2011 The sequence read archive. Nucleic Acids Res. 39: D19–D21. https://doi.org/10.1093/nar/gkq1019

Lindholm, A. K., K. A. Dyer, R. C. Firman, L. Fishman, W. Forstmeier *et al.*, 2016 The ecology and evolutionary dynamics of meiotic drive. Trends Ecol. Evol. 31: 315–326. https://doi.org/10.1016/j.tree.2016.02.001

Liu, H., Q. Wang, Y. He, L. Chen, C. Hao *et al.*, 2016 Genome-wide A-to-I RNA editing in fungi independent of ADAR enzymes. Genome Res. 26: 499–509. https://doi.org/10.1101/gr.199877.115

Liu, H., Y. Li, D. Chen, Z. Qi, Q. Wang *et al.*, 2017 A-to-I RNA editing is developmentally regulated and generally adaptive for sexual reproduction in *Neurospora crassa*. Proc. Natl. Acad. Sci. USA 114: E7756–E7765. https://doi.org/10.1073/pnas.1702591114

Lyon, M. F., 2003 Transmission ratio distortion in mice. Annu. Rev. Genet. 37: 393–408. https://doi.org/10.1146/annurev.genet.37.110801.143030

Marchler-Bauer, A., M. K. Derbyshire, N. R. Gonzales, S. Lu, F. Chitsaz *et al.*, 2015 CDD: NCBI's conserved domain database. Nucleic Acids Res. 43: D222–D226. https://doi.org/10.1093/nar/gku1221

Margolin, B. S., M. Freitag, and E. U. Selker, 1997 Improved plasmids for gene targeting at the *his-3* locus of *Neurospora crassa* by electroporation. Fungal Genet. Newsl. 44: 34–36.

McCluskey, K., A. Wiest, and M. Plamann, 2010 The fungal genetics stock center: a repository for 50 years of fungal genetics research. J. Biosci. 35: 119–126. https://doi.org/10.1007/s12038-010-0014-6

McLachlin, D. T., and S. D. Dunn, 1997 Dimerization interactions of the b subunit of the *Escherichia coli* F_1F_0-ATPase. J. Biol. Chem. 272: 21233–21239. https://doi.org/10.1074/jbc.272.34.21233

Nuckolls, N. L., M. A. B. Núñez, M. T. Eickbush, J. M. Young, J. J. Lange *et al.*, 2017 *wtf* genes are prolific dual poison-antidote meiotic drivers. Eng. Life Sci. 6: e26033.

Perkins, D. D., 1974 The manifestation of chromosome rearrangements in unordered asci of Neurospora. Genetics 77: 459–489.

Raju, N. B., 1979 Cytogenetic behavior of Spore killer genes in Neurospora. Genetics 93: 607–623.

Raju, N. B., 1980 Meiosis and ascospore genesis in Neurospora. Eur. J. Cell Biol. 23: 208–223.

Raju, N. B., 1994 Ascomycete spore killers: chromosomal elements that distort genetic ratios among the products of meiosis. Mycologia 86: 461–473. https://doi.org/10.1080/00275514.1994.12026437

Raju, N. B., D. D. Perkins, and D. Newmeyer, 1987 Genetically determined nonselective abortion of asci in *Neurospora crassa*. Can. J. Bot. 65: 1539–1549. https://doi.org/10.1139/b87-212

Raju, N. B., R. L. Metzenberg, and P. K. T. Shiu, 2007 Neurospora Spore killers *Sk-2* and *Sk-3* suppress meiotic silencing by unpaired DNA. Genetics 176: 43–52. https://doi.org/10.1534/genetics.106.069161

Revington, M., D. T. McLachlin, G. S. Shaw, and S. D. Dunn, 1999 The dimerization domain of the b subunit of the *Escherichia coli* F(1)F(0)-ATPase. J. Biol. Chem. 274: 31094–31101. https://doi.org/10.1074/jbc.274.43.31094

Rhoades, M., 1952 Preferential segregation in maize, pp. 66–80 in *Heterosis: A Record of Researches Directed Towards Explaining and Utilizing the Vigor of Hybrids*, edited by J. W. Gowen. Iowa State College Press, Ames, IA.

Samarajeewa, D. A., P. A. Sauls, K. J. Sharp, Z. J. Smith, H. Xiao *et al.*, 2014 Efficient detection of unpaired DNA requires a member of the Rad54-like family of homologous recombination proteins. Genetics 198: 895–904. https://doi.org/10.1534/genetics.114.168187

Saupe, S. J., 2011 The [Het-s] prion of *Podospora anserina* and its role in heterokaryon incompatibility. Semin. Cell Dev. Biol. 22: 460–468. https://doi.org/10.1016/j.semcdb.2011.02.019

Shiu, P. K. T., N. B. Raju, D. Zickler, and R. L. Metzenberg, 2001 Meiotic silencing by unpaired DNA. Cell 107: 905–916. https://doi.org/10.1016/S0092-8674(01)00609-2

Shiu, P. K. T., D. Zickler, N. B. Raju, G. Ruprich-Robert, and R. L. Metzenberg, 2006 SAD-2 is required for meiotic silencing by unpaired DNA and perinuclear localization of SAD-1

RNA-directed RNA polymerase. Proc. Natl. Acad. Sci. USA 103: 2243–2248. https://doi.org/10.1073/pnas.0508896103

Stewart, A. G., E. M. Laming, M. Sobti, and D. Stock, 2014 Rotary ATPases–dynamic molecular machines. Curr. Opin. Struct. Biol. 25: 40–48. https://doi.org/10.1016/j.sbi.2013.11.013

Sugimoto, M., 2014 Developmental genetics of the mouse *t*-complex. Genes Genet. Syst. 89: 109–120. https://doi.org/10.1266/ggs.89.109

Svedberg, J., S. Hosseini, J. Chen, A. A. Vogan, I. Mozgova *et al.*, 2018 Convergent evolution of complex genomic rearrangements in two fungal meiotic drive elements. Nat. Commun. 9: 4242. https://doi.org/10.1038/s41467-018-06562-x

Thompson, J. D., D. G. Higgins, and T. J. Gibson, 1994 CLUSTAL W: improving the sensitivity of progressive multiple sequence alignment through sequence weighting, position-specific gap penalties and weight matrix choice. Nucleic Acids Res. 22: 4673–4680. https://doi.org/10.1093/nar/22.22.4673

Turner, B. C., 2001 Geographic distribution of *Neurospora* Spore killer strains and strains resistant to killing. Fungal Genet. Biol. 32: 93–104. https://doi.org/10.1006/fgbi.2001.1253

Turner, B. C., and D. D. Perkins, 1979 Spore killer, a chromosomal factor in Neurospora that kills meiotic products not containing it. Genetics 93: 587–606.

Vogel, H. J., 1956 A convenient growth medium for Neurospora (Medium N). Microb. Genet. Bull. 13: 42–43.

Walker, J. E., M. Saraste, and N. J. Gay, 1984 The *UNC* operon nucleotide sequence, regulation and structure of ATP-synthase. Biochim. Biophys. Acta 768: 164–200. https://doi.org/10.1016/0304-4173(84)90003-X

Wang, Y., K. M. Smith, J. W. Taylor, M. Freitag, and J. E. Stajich, 2015 Endogenous small RNA mediates meiotic silencing of a novel DNA transposon. G3 (Bethesda) 5: 1949–1960. https://doi.org/10.1534/g3.115.017921

Westergaard, M., and H. K. Mitchell, 1947 Neurospora V. A synthetic medium favoring sexual reproduction. Am. J. Bot. 34: 573–577. https://doi.org/10.1002/j.1537-2197.1947.tb13032.x

Yu, J. H., Z. Hamari, K. H. Han, J. A. Seo, Y. Reyes-Domínguez *et al.*, 2004 Double-joint PCR: a PCR-based molecular tool for gene manipulations in filamentous fungi. Fungal Genet. Biol. 41: 973–981. https://doi.org/10.1016/j.fgb.2004.08.001

Zimmering, S., L. Sandler, and B. Nicoletti, 1970 Mechanisms of meiotic drive. Annu. Rev. Genet. 4: 409–436. https://doi.org/10.1146/annurev.ge.04.120170.002205

Communicating editor: D. Barbash